DETERMINATION OF SEA LEVEL TRENDS AND VERTICAL LAND MOTIONS FROM SATELLITE ALTIMETRY AND TIDE GAUGE OBSERVATIONS AT THE MEDITERRANEAN COAST OF TURKEY

A THESIS SUBMITTED TO
THE GRADUATE SCHOOL OF NATURAL AND APPLIED SCIENCES
OF
MIDDLE EAST TECHNICAL UNIVERSITY

BY

SITAR KARABİL

IN PARTIAL FULFILLMENT OF THE REQUIREMENTS
FOR
THE DEGREE OF MASTER OF SCIENCE
IN
GEODETIC AND GEOGRAPHIC INFORMATION TECHNOLOGIES

DECEMBER 2011

Approval of the thesis:

DETERMINATION OF SEA LEVEL TRENDS AND VERTICAL LAND MOTIONS FROM SATELLITE ALTIMETRY AND TIDE GAUGE OBSERVATIONS AT THE MEDITERRANEAN COAST OF TURKEY

Submitted by **SITAR KARABİL** in partial fulfillment of the requirements for the degree of **Master of Science in Geodetic and Geographic Information Technologies Department, Middle East Technical University** by,

Prof. Dr. Canan Özgen _____
Dean, Graduate School of **Natural and Applied Sciences**

Assoc. Prof. Dr. Ayşegül Aksoy _____
Head of Dep., **Geodetic and Geographic Info. Technologies**

Prof. Dr. Mahmut Onur Karslıoğlu _____
Supervisor, **Civil Engineering Department, METU**

Dr. Coşkun Demir _____
Co-Supervisor, **General Command of Mapping - Retired**

Examining Committee Members:

Assoc. Prof. Dr. Zuhal Akyürek _____
Civil Engineering Department, METU

Prof. Dr. Mahmut Onur Karslıoğlu _____
Civil Engineering Department, METU

Dr. Coşkun Demir _____
General Command of Mapping - Retired

Assoc. Prof.Dr. Ali Kılıçoğlu _____
General Command of Mapping - Retired

Assoc. Prof. Dr. Mehmet Lütfi Süzen _____
Geological Engineering Department, METU

Date: 16/ 12/2011

I here by declare that all information in this document has been obtained and presented in accordance with academic rules and ethical conduct. I also declare that, as required by these rules and conduct, I have fully cited and referenced all material and results that are not original to this work.

Name, Last Name: Sıtar Karabil

Signature:

ABSTRACT

DETERMINATION OF SEA LEVEL TRENDS AND VERTICAL LAND MOTIONS FROM SATELLITE ALTIMETRY AND TIDE GAUGE OBSERVATIONS AT THE MEDITERRANEAN COAST OF TURKEY

Karabil, Sıtar
M.Sc., Department of Geodetic and Geographic Info. Technologies
Supervisor: Prof. Dr. Mahmut Onur Karslıoğlu
Co-Supervisor: Dr. Coşkun Demir

December 2011,103 Pages

A radar altimetry satellite measures the height of sea surface globally. However, tide gauges, measuring Sea Level Height (SLH), are set up on the Earth surface. Hence, SLHs are involved in vertical motion of the Earth crust. In this study, vertical motions of Earth crust have been separated from sea level variations.

After clustering of SSH observations with K-means approach, two outlier detection methods Pope and Interquartile (IQR) Tests are implemented in data. Afterwards, each altimetry measurement is relocated to the center point of own cluster by means of geoid height derived from Earth Gravitational Model 2008 (EGM08). Before application of Principal Component Analysis (PCA) to see behavior of SSH inbetween clusters, Lomb Scargle algorithm is run to realize power spectrum of every clustered observations distinctly.

Besides, tide gauge measurements are used for extracting 68 constituents with T_Tide program from hourly tide gauge observations. Then, predicted signal is produced by means of classical tidal harmonic analysis. To get monthly and daily mean values of hourly data, MSDOS

Processing and Quality Controlling Software (SLPR2) has been run and the results are compared with Permanent Service for Mean Sea Level (PSMSL) monthly mean sea level values. Afterwards, the trends from altimetry, tide gauge and GPS are investigated to reveal vertical land motion.

This study shows that sea level is rising every year more or less 7 mm at the Mediterranean coast of Turkey. Although İskenderun tide gauge subsides 50 mm every year, the other stations do not show huge amount of vertical motion.

Keywords: Satellite Altimetry, Tide Gauge, Sea Level Trends, Vertical Motion.

öz

UYDU ALTİMETRESİ VE MAREOGRAF İSTASYONLARI GÖZLEMLERİ İLE TÜRKİYE'NİN AKDENİZ KIYISINDA DENİZ SEVİYESİ TRENDLERİNİN VE DÜŞEY YER KABUĞU HAREKETLERİNİN BELİRLENMESİ

Karabil, Sıtar
Yüksek Lisans, Jeodezi ve Coğrafi Bilgi Teknolojileri
Tez Yöneticisi: Prof. Dr. Mahmut Onur Karslıoğlu
Ortak Tez Yöneticisi: Dr. Coşkun Demir

Aralık 2011,103 Sayfa

Bir radar altimetre uydusu Deniz Yüzeyi Yüksekliği'ni (DYY) global olarak ölçer. Ancak, Deniz Seviyesi Yüksekliği'ni (DSY) ölçen mareograf istasyonları yeryüzeyi üzerine kurulmuştur. Bu nedenle DSY verileri yer kabuğunun düşey hareketini de içerir.Bu çalışmada, yer kabuğunun düşey hareketleri deniz seviyesi değişimlerinden ayrıştırılmıştır.

DYY gözlemlerinin K-means yaklaşımıyla kümelendirilmesinden sonra uyuşumsuz ölçülerin tespiti için veri Pope ve interkartil testleri yapılmıştır. Daha sonra, her bir altimetre ölçüsü Yer Gravite Modeli 2008 (YGM08)'den elde edilen geoid yükseklikleri aracılığıyla kendi kümesinin merkez noktasına taşınmıştır. DYY'nin kümeler arasındaki davranışını ortaya koymak için Temel Bileşenler Analizi (TBA) uygulanmadan önce kümelenmiş her gözlemin güç spekturumu Lomb Algoritması yürütümü ile açık bir şekilde ortaya konmuştur.

Bununla birlikte, saatlik mareograf deniz seviyesi gözlemleri kullanılarak 68 adet gelgit bileşeni T_Tide program ile elde edilmiştir. Daha sonra klasik gelgitsel harmonik analiz kullanılarak kestirim sinyali üretilmiştir. Saatlik deniz seviyesi gözlemlerinden günlük ve aylık deniz seviyesi değerleri elde etmek için SLPR2 yazılımı kullanılarak sonuçlar PSMSL'den elde edilen aylık ortalama değerlerle kıyaslanmıştır. Son olarak, düşey yer kabuğu hareketlerini ortaya çıkarmak için altimetri, mareograf ve GPS trendleri irdelenmiştir.

Bu çalışma Türkiye'nin Akdeniz kıyısında her yıl 7 mm civarında bir deniz seviyesi artışı olduğunu göstermektedir. Her ne kadar İskenderun mareograf istasyonunda yıllık 50 mm'lik bir çöktüğü tespit edilse de diğer istasyonlarda büyük bir düşey hareket görülmemektedir.

Anahtar Kelimeler: Uydu Altimetresi, Mareograf, Deniz Seviyesi Trendleri, Düşey Hareket.

To My Mother and My Deary Friend Kamuran Çakır

ACKNOWLEDGEMENTS

I am greatly indebted to Mahmut Onur Karslıoğlu for his supervision, friendly and wisdom advices and scientific suggestions which give direction to my studies.

I am also indebted to Coşkun Demir for his supports and encouragements, which helped me whenever I felt hopeless. I have enormously benefited from his scientific teachings and minded arguments on the data processing.

Special thanks go to Ali Kılıçoğlu for his support and encouragement and for sharing his profound knowledge in related subjects of this thesis.

I also thank to examining committee members Zuhal Akyürek, Mehmet Lütfi Süzen for their valuable comments and contributions.

I would like to take this opportunity to thank Civil Engineering Department, Geomatics Division participants for their understanding and contributions during my thesis studies, especially my roommate Armin Aghakarimi.

Last but not least, I would like to express my deepest thanks to Eren Erdoğan and Özkan Yılmaz who have not left me lonely in any challenging condition since 2005.

TABLE OF CONTENTS

LIST OF TABLES

TABLES

LIST OF FIGURES

FIGURES

CHAPTER 1

INTRODUCTION

1.1 Background

Altimetry satellites were started to be launched in the early 1970s. First mission called Skylab was launched in May 1973. Then, the other altimetry satellites are succeeded such as GEOSAT, ERS-1.TOPEX/POSEIDON, GFO, ERS-2, Jason-1. ENVISAT, Jason-2, and also six more satellites will be on duty in the near future (Benveniste and Picot 2011).

A radar altimeter obtains data about the shape of the Earth globally. These measurements give rise to perform different kind of altimetry applications such as geodesy, geophysics, ocean, ice, climate, atmosphere, wind, waves, hydrology and coastal studies. It is generally known that geodesy is the science of the Earth's shape and size. If the matter of geodesy is to determine external gravity field of the Earth, it can be said that the precise knowledge of the physical size and shape of the sea surface is an important factor of the problem. If the problem of physical oceanography is to monitor the temporal variations of the sea surface, a global high-accuracy high-resolution mean sea surface (MSS) model can play key role in absolute oceanic datum for this purpose. Satellite altimetry measures the real shape of the oceans directly. The precision of altimeter SSHs has progressed from SKYLAB to the TOPEX/POSEIDON. The accuracy and resolution of MSS models have been improved across all spatial and temporal scale by means of better

precision and spatial coverage of the altimeter measurements (Fu and Cazenave 2001).

A tide gauge measures sea level height (SLH) at the coastline fixed to the Earth surface. As a result of continuously observation of sea level, tide gauge measurements can be used in the area of geodesy, geophysics, geology, oceanography, climatology, meteorology, water resource management, hydrology, sailing, coastal risk management, human and environmental security in order to run different applications related with water ascent and descent. There are more than two thousand tide gauges over the world (PSMSL 2011).

Turkey, with responsibility of General Command of Mapping (GCM) has eleven tide gauges. Basically tide gauge network is to define SLH at the coastal line. The first tide gauge station was set up at Antalya Harbor in 1936. After that date there were some studies to define zero level for national vertical control network in Turkey. At present Turkish National Sea Level Monitoring System (TUSELS) has Ankara data center and tide gauge stations namely Antalya-II, Erdemli, Bozyazı, Taşucu, İskenderun, Girne, Bodrum-II, Menteş, Erdek, Amasra, Trabzon-II, İğneada, Sinop, Gökçeada, Şile, Marmara Ereğlisi, Aksaz, Gazimağusa and Şile (Yıldız, et al. 2003), (H. Yıldız 2001).

Since tide gauge measures the relative motion between sea surface and the ground where station is located at, the problem of relative motion must be eliminated to use SLH meaningfully (H. Yıldız 2001), (Carrera and Vanicek 1985). To separate sea level change resulting from sea level variations from vertical land motion, it can be said that analysis of sea level variations does not give sufficient results before correcting them with external source like satellite altimetry data. Sea level trends are also useful to define vertical crustal motion, if ancillary information source is considered (Carrera and Vanicek 1985), (IOC 2000).

Long-term sea-level change has been estimated from tide gauge measurements more than the last century. However, two fundamental problems have been come out when using tide gauge measurements for this purpose. First, tide gauges only measure sea level change relative to a crustal reference point, which may move vertically at rates comparable to the true sea-level signals (Douglas 1995). Second, tide gauges have limited spatial distribution and suboptimal coastal locations, and thus they provide poor spatial sampling of the SSH (T. Barnett 1984), (Groger and Plag 1993).

An independent global measurement technique is needed to investigate the important issues associated with SSH change. In principle, satellite altimeters should provide improved measurements of global sea-level change over shorter averaging periods because of their truly global coverage and direct tie to the Earth's center of mass (Fu and Cazenave 2001).

Satellite altimeters provide a measure of absolute sea level relative to a precise reference frame realized through the satellite tracking stations whose origin coincides with the Earth's center of mass (Nerem, et al. 1998).

(Marc, Dietz and Groten 2004) have computed estimates of the rate of vertical land motion in the Mediterranean Sea from differences of sea heights measured by the TOPEX/Poseidon radar altimeter and by a set of tide gauge stations. Afterwards, they have predicted absolute vertical land motion in the Mediterranean Sea relative to the geocenter by computing the linear term of the differences of altimetry and tide gauges SLH time series.

Additionally, (Kuo and Shum 2004) have shown some combining results regarding the subject. They presented a new method of combining satellite altimetry and tide gauge data to obtain improved estimates of absolute vertical crustal motion at tide gauges within a semi-enclosed

sea. As an illustration, they have combined T/P altimetry data and 25 tide gauge records around the Baltic Sea Region of Fennoscandia.

(Garcia, et al. 2007) compared tide gauge data with SSH anomaly obtained from T/P and ERS-1/2 for a period of 1993-2001. They have estimated vertical ground motion, for each tide gauge, from the slope of the SSH time series of the difference between records and the altimetry measurement at a point closest to the tide gauge.

(Mitchum 1994) studied on comparison of tide gauge and altimetry measurements with some statistical assessments. Then, Mitchum has reached some results regarding tidal constituents and precision of measurements. On the other hand, (C. Kuo, et al. 2008) presented a new robust technique to estimate absolute vertical motion using both satellite altimetry and tide gauge records in Fennoscandia, Alaskan coast, and the Great Lakes.

(Nerem and Mitchum 2002) have computed estimates of the rate of vertical crustal motion from differences of sea level measurements made by the TOPEX/POSEIDON radar altimeter and a globally distributed network of 114 tide gauges. In that study, a rigorous error analysis was performed which suggests the accuracy of the estimated vertical rates is approximately 1-2 mm/year for roughly half of the tide gauges, which is sufficiently accurate to detect a variety of geophysical phenomena.

Moreover, (Braitenberg, et al. 2010) examined tide gauge and satellite altimetry observations of sea level with the aim of obtaining crustal vertical movement rates. The correction of the tide gauge data sea level rates for the SSH contribution requires collocation of the satellite pass and the tide gauge station. They showed that the satellite altimetry observations enable correction of differential tide gauge rates for the effects of sea surface rate inhomogenities. Coastal sea level trends can be defined with the comparison of altimetry and tide gauge observations.

(Mangiarotti 2007)has made a joint analysis with using T/P satellite altimetry and tide gauge data to estimate sea level trends along the Mediterranean Sea coast from 1993 January to 2002 February. To detect long-term sea level change, (L. F. Marc 2002) has gathered data of T/P, ERS-1/2 missions and from tide gauge data. In that study, long-term sea level change during 1992-2000 is investigated in the Mediterranean Sea.

1.2 Motivation

In this study, T/P, Jason-1 satellite missions are used to extract altimetry measurements from Basic Radar Altimetry Toolbox (BRAT) which is developed by European Space Agency (ESA) and Centre National d'Etudes Spatiales (CNES). The data is obtained from Archiving, Validation and Interpretation of Satellite Oceanographic Data (AVISO).

After getting the proper data according to its space and time, processes have been implemented in MATLAB R2010b. These processes include

- clustering of data,
- outlier detection tests and comparisons of methods,
- significant test of parameters,
- interpolation of SSHs with respect to their spatial distribution with the aid of geoid height,
- spectral and time domain analysis of altimetry data,
- Principle Component Analysis (PCA) of altimetry data,
- Determination of SSH trends.

To get the geoid height, Earth Gravitational Model 2008 (EGM08) has been taken as the model.

Tide gauge data have been obtained from GCM. Within this study four tide gauge stations have been used to investigate sea level trends and vertical land motions of tide gauge stations. Tide gauge hourly data is analyzed with classical tidal harmonic analysis model, then significant

tidal constituents have been defined to get predicted signal (Pawlowicz, Beardsley and Lentz 2002). Predicted signal is needed to full data gaps in hourly data. Hourly data, to be able to compare with altimetry observations, has been filtered to make it for daily and monthly data with the help of SLPR2 software ((SLC) 2011).

Afterwards, SSH trends are extracted from the information of similarity percentage derived from PCA method on altimetry observations. Since sea surface is assumed as homogenous in small area, the most common group of cluster has been considered to compute SSH trends. Also, almost all clusters, excluding last three clusters, have been taken into account to calculate SSH trends of each Pass. Then, difference rates of SSHs-SLHs are defined to be able to figure out sea level trends and vertical crustal movements of tide gauge stations. To see the SSH trends of each Pass, for the SSH trend derived from chosen clusters, arithmetic mean of chosen clusters is accepted as SSH trend. On the other hand, at the second approach only excepting last three clusters, SSH trend has been calculated from linear regression of first principal component.

The scope of this study is to find mainly vertical crustal motion of the Bodrum, Antalya, Erdemli and İskenderun tide gauges and partly SSH and SLH trends on the North Eastern Mediterranean Sea. The flowchart of this study can be seen in Figure 1.

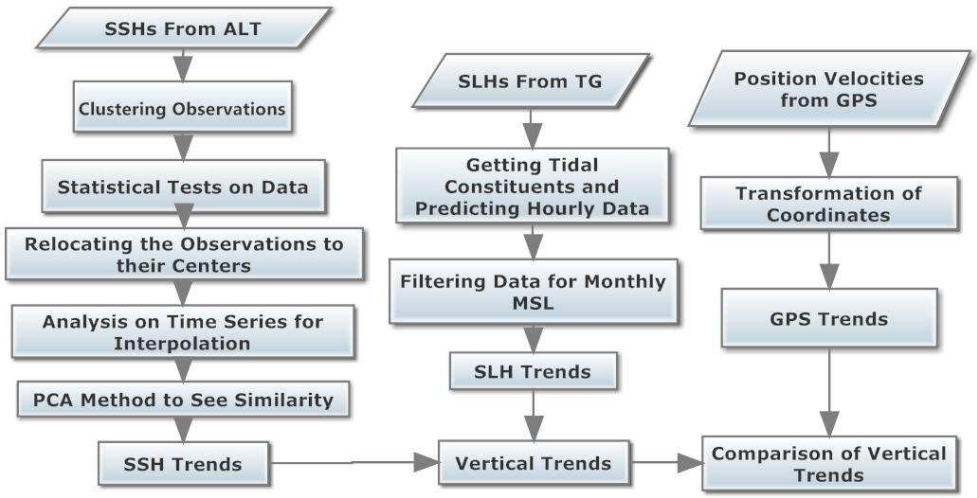

Figure 1 Flowchart of the Study

1.3 Study Area

Study area is located roughly between 35°N-37°N latitude, and 27°E-36°E longitude. This means thatstudy area is North-Eastern Mediterranean Sea, especially the Mediterranean coast of Turkey.

In this study, the tracks of T/P and Jason-1 like 68, 159, 170 and 246 have been chosen for Erdemli, İskenderun, Bodrum and Antalya respectively. Tide gauge stations can be seen in Figure 2.

Figure 2 Tide Gauge Stations

Theoretical tracks of altimetry missions are shown in Figure 3.

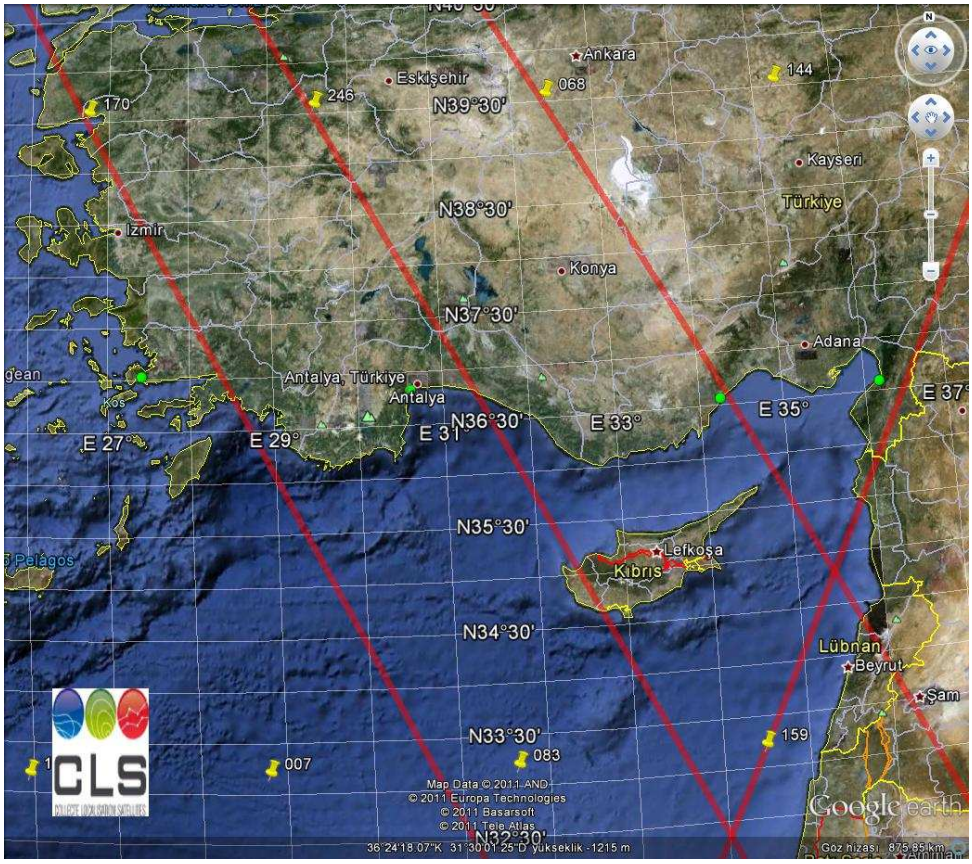

Figure 3 Chosen Theoretical Tracks

1.4 Thesis Outline

This thesis consists of seven chapters. Background and objectives of study are explained in Chapter1.

Chapter 2 is dedicated to give brief information about satellite altimetry and its missions, used software, products and content of data which are obtained by a mission.

Quality control, interpolation and analysis of altimetry data are handled in Chapter 3. As subtopic, BIN method and clustering are mentioned, and statistical tests have been applied to data with detection of outlier and significance of trend parameters. Each altimetry measurement is brought to its center with respect to geoid undulation. Afterwards, time domain and frequency domain analysis have been implemented in SSH data for interpolation detailed in this chapter. Lastly, evaluation of PCA is the result of this chapter.

Tide gauge data and related products are presented in Chapter 4. Also, to define tidal constituents and fulfill data gaps, harmonic analysis has been applied to hourly data.

Determining Vertical Trends, Chapter 5, which covers determination of vertical trends and extracting crustal motions on the tide gauges are contained. SSH trends and SLH trends have been defined and compared to see the vertical trends and vertical crustal motion for each tide gauge points. Also, brief information about GPS technique is given here.

The results are discussed and evaluated in Chapter 6. Within this purpose results are investigated in different views.

A concluding remark and future works are indicated in Chapter 7 with a summary.

CHAPTER 2

SATELLITE ALTIMETRY

2.1 Introduction

Altimetry is a kind of technique for measuring SSH directly according to a reference frame. Satellite radar altimetry measures time of a signal produced by a radar pulse round-trip from the satellite to surface of the Earth and return to the receiver of the same satellite. Moreover, this measurement yields amount of other information that can be used for a wide range of applications.

The principle is that the altimeter emits a radar wave and analysis the bounced off signal from the Earth surface. SSH is the difference between position of satellite with respect to an arbitrary reference surface (altitude) and satellite-to-surface distance (range) calculated by measured time. The time is period of signal between satellite and the Earth round trip. Besides SSH, by looking at the return signal's amplitude and waveform, we can also measure wave height and wind speed over the oceans, backscatter coefficient and surface roughness.

If the altimeter emits in two frequencies, the comparison between the signals, with respect to the used frequencies, can also generate interesting results like rain ratio on the oceans, over ice shelves, detection of crevasses etc.

To obtain accurate measurements within a few centimeters from a range of several hundred kilometers requires an extremely precise knowledge

of the satellite position. Thus several locating systems are usually embedded onboard altimetry satellites. Any interference with the radar signal also needs to be taken into account. Water vapor and electrons in the atmosphere, sea state and a range of other parameters can affect the signal travel time, thus distorting range measurements. We can correct these interference effects on the altimeter signal by measuring them. There are three main methods to bring correction on these effects like embedding supporting instruments into satellite, using several different frequencies on satellite, modeling the effects.

Altimetry requires an amount of information to be considered before being able to use the data. Namely, data preprocessing is also a major part of altimetry, producing data of different levels optimized for different uses.

Radar altimeters on board the satellite transmit signals at high frequencies (over 1.700 pulses per second) to Earth, and receive the echo from the surface. This is analyzed to derive a precise measurement of the time taken to make the round trip between the satellite and the surface. This time measurement, scaled to the speed of light, the speed at which electromagnetic waves travel, yields a range R measurement. The ultimate aim is to measure surface height relative to a terrestrial reference frame. The principal of satellite altimetry can be seen in Figure 4 (Benveniste and Picot 2011).

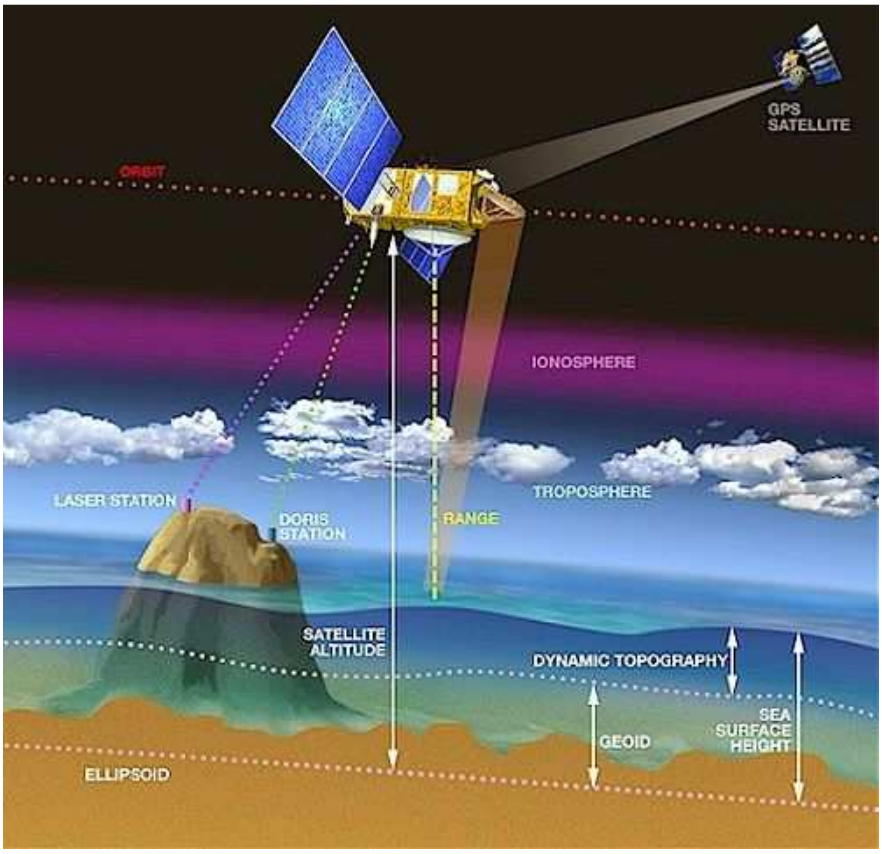

Figure 4 Principle of Radar Altimetry (Benveniste and Picot 2011)

The important parameters of orbit for satellite altimeter missions are inclination, altitude, and period. The period is the time needed for the satellite to pass over the same position on the Earth surface. Inclination gives the highest latitude where the satellite can measure the Earth.

The altitude of a satellite is the distance of satellite with respect to a predefined reference surface. It is up to amount of limitations like inclination, atmospheric drag, gravity forces, field of the world to be mapped. The satellite can be tracked in several approaches to measure its altitude with the best possible accuracy, so determine its precise orbit, accurate within 1 or 2 cm. So that SSH measurement can reach toapproximately 4 cm accuracy for both T/P and Jason-1.To achieve the

goal for SSH accuracy (2.5 cm root-mean-square -RMS), radial orbit errors must be reduced to 1 cm (RMS) (CalVal, AVISO 2011).

The SSH is the distance of satellite at a measurement time from the defined reference surface, so:

SSH = Satellite Altitude – (Altimeter Range + Corrections).

To deduce the dynamic topography, the easiest solution could be to subtract the geoid height from SSH. But in practice, mean sea level is subtracted, to determine the sea level anomalies of the ocean signal.

Several different frequencies are used for radar altimeters. The choice depends upon regulations, mission objectives and constraints and technical possibilities. Each frequency band has its advantages and disadvantages. These bands are Ku band (13.6 GHz),C band (5.3 GHz),S band (3.2 GHz),Ka band (35 GHz). (Benveniste and Picot 2011)

2.2 Missions

Missions classification can be made based on the expire and launch date of them. With this point of view there are three main parts to mention: past missions, current missions and future missions. While Geosat, ERS-1, Topex/Poseidon, GFO are past missions, ERS-2, Jason-1, Envisat, Jason-2, Cryosat are present missions. Scheduled future missions are Saral, HY-2, Sentinel 3, Jason-3. The missions are detailed in following table, Table 1 (Benveniste and Picot 2011).

Table 1 Altimetry Missions (Benveniste and Picot 2011)

Satellite	*Launch*	*Mission*	*Frequency*	*Altitude*	*Inclination*
SkyLab	1973	Acquiring new knowledge in Space to improve life on Earth		435 km	50°
GEOS 3	1975	Geodesy		845 km	115°
Seasat	1978	Study Earth and its Seas	Ku Band	800 km	108°
Geosat	1985	Describing marine geoid	Ku Band	800 km	108°
ERS-1	1991	Observe Earth and its Environment	Ku Band	785 km	98.5°
T/P	1992	Measure SSH	Ku-C Band	1336 km	66°
GFO	1998	Measure ocean topography	Ku Band	800 km	108°
ERS-2	1995	Observe Earth and its Environment	Ku Band	785 km	98.52°
Jason-1	2001	Measure SSH	Ku-C Band	1336 km	66°
Envisat	2002	Observe Earth's atmosphere and surface	Ku-S Band	800 km	98.5°
Jason-2	2008	Measure SSH	Ku-C Band	1336 km	66°
Cryosat	2010	Polar observation	Ku Band	720 km	92°
Saral	2012	Measure SSH	Ka Band	800 km	92°
HY-2	2011	Observe the ocean dynamics	Ku-C Band	963 km	99.3°
Sentinel 3	2013	Provide operational oceanography data for GMES	Ku-C Band	814 km	98.5°
Jason-3	2013	Measure SSH	Undefined dual frequency	1336 km	66°

By means of satellite altimetry missions, we are able to view the Earth and its open and semi-closed seas from the vantage point in space. Thus, measurements obtained from altimetry missions give an advantage to observe sea surface of Earth globally and frequently.

2.3 Products of Altimetry Missions

There is wide range of data and software to be used in altimetry applications. Products as data can be derived from an altimetry mission. These products generally are sea surface height, significant wave height, sea surface height anomaly, sea level anomaly, bathymetry, sea surface temperature, range, mean sea surface, wind speed and dynamic ocean topography. Additionally, gravitational potential and regarding products, like disturbing potential, gravity, gravity anomaly, gravity gradiant, can be derived from sea surface height information in different platforms like Geopot 2007.

In addition to data product, there is a broad range of software to be used in altimetry applications. Basic Radar Altimetry Toolbox (BRAT), PublicReadBinaries, SSHA software, OPR reading software, Modified Chelton-Wentz model, EnviView, Envisat L2 RA2-MWR Products Read and Write Software and Convert programs for waveforms POSEIDON products can be emphasized as main altimetry software products (Benveniste and Picot 2011).

2.4 Used Missions and Data

Considering study area and time span, two different altimetry missions are chosen to obtain altimetry data. These missions are Jason-1and Topex/Poseidon. Additionally, BRAT developed by CNES and ESA is taken as altimetry software product within this study. Besides, AVISO corrected SSH data obtained from (AVISO 2011) is explained below in Table 2. The altimeter products were produced by CLS Space Oceanography Division and distributed by AVISO, with support from CNES.

Table 2 Used Data from AVISO

Satellite	Data Time Interval	Data Period
Jason-1	February 2002 – January 2009	10 days
T/P	January 1999 – February 2002	10 days

Altimetry measurements need to be corrected for instrumental errors, environmental perturbations like wet tropospheric, dry tropospheric and ionospheric effects. Also, the ocean sea state influence, the tide influence and atmospheric pressure must be considered to be corrected. With this aim AVISO has brought the most renewed residuals into altimetry data. Thus, the applied residuals are orbit, dry troposphere, wet troposphere, Ionosphere, sea state bias, ocean and loading tides, solid Earth tide, pole tide, combined atmospheric correction, major instrumental correction (H. AVISO 2011).

In this study, these data are processed in BRAT software. As mentioned above, BRAT software is advanced with the responsibility of ESA/CNES. BRAT is a tool to run the processing of radar altimetry data. Besides, BRAT is able to treat so many radar altimetry data formats, providing support for processing, editing, extracting statistics, visualizing and exporting the outputs.

BRAT covers some modules operating at different levels of abstraction. These modules can be Graphical User Interface (GUI) applications, command-line tools, interfaces to applications like MATLAB or application program interfaces (APIs) to programming languages such as C and Fortran (ESA and CNES 2011). Sample outputs of BRAT are given in Figure 4.

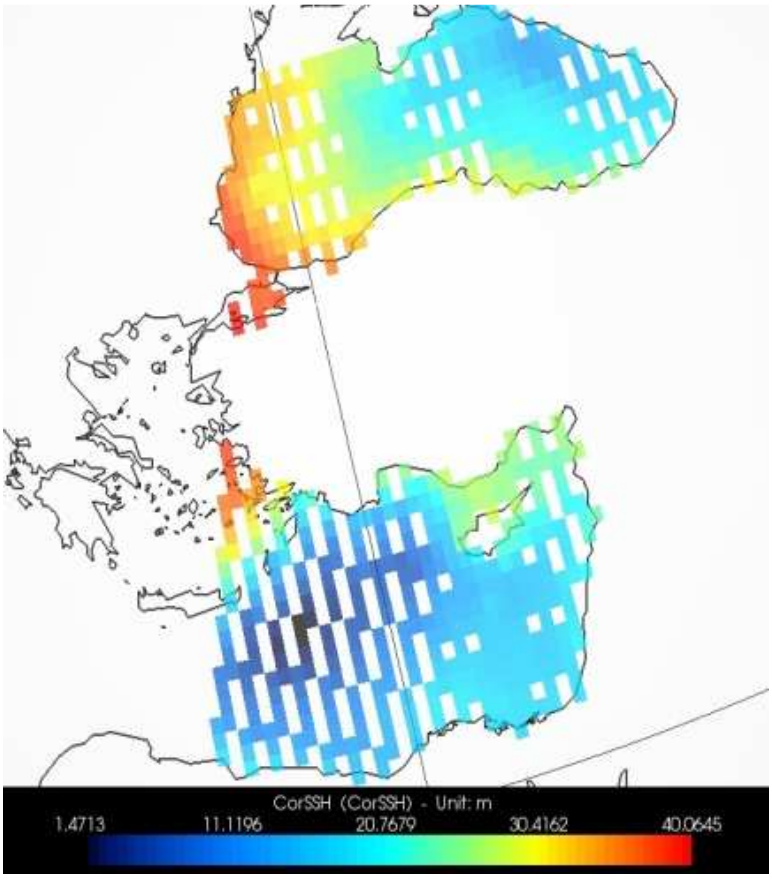

Figure 5 Sample Satellite Tracks Produced by BRAT

CHAPTER 3

QUALITY CONTROL, ANALYSIS AND INTERPOLATION OF ALTIMETRY DATA

3.1 Creating BIN and Clustering of Observations

BIN data structure developed by (Bosch and Savcenko 2005) is the reorganization of satellite altimeter data to perform time series analysis. BINs are clusters along ground track of the altimeter satellite. Their positions are defined according to equator crossing of the ground track of altimeter satellite. To be able to have at least one observation, each BIN is separated by 1 Hz which means 7 km distance.

Numbering of BINs is given by bin Id number. This Id number is defined with respect to the equator crossing. binid = 0 means that the center of that BIN is crossing of the equator with the ground track. For ascending satellite pass BIN numbers are negative at the south of the equator, and BINs are positive at the north of the equator. Besides, for the descending pass of any satellite mission vice versa.

For example, BINs are divided into 3101 parts from -1500 to +1500. For ascending pass of T/P first number will be -1500 and last number will be -1 before the equator, and it continues with the same approach for north side of the equator (Bosch and Savcenko 2005).

In this study, BIN data structure is handled as a sample method to explain clustering sense of SSH data. To cluster the data K-means

approach has been applied. The K-means algorithm, very popular to cluster the data, is developed by (MacQueen 1967) in 1967. K-means searches for a proper segment of the data by minimizing the sum-of-squared-error criterion with an iterative procedure (Xu ve Wunsch II 2009). The important part of this clustering method is to define distance between data. K-means algorithm can compute similarity of 2D and 3D data geometrically. Definition of cluster number is the weak point of K-means algorithm because of depending on user's choice. However, ISODATA approach is introduced by (Ball and Hall 1967) deals with dynamic prediction of cluster number. The steps of K-means clustering method can be summarized as below.

i. Cluster centers are defined according to cluster numbers,
ii. The distance of each single point from each center is computed. Then, all the data points are put into the clusters according to the closest distance,
iii. Each center point of clusters is calculated again by means of averaging of positions of all data points in cluster. Old center point is relocated with the new one,
iv. Iterative computation in (ii) and (iii) arerepeated again till new center point remains the same with previous one.

Each mission is clustered within this concept by means of generating the required codes in MATLAB R2010b platform (Govaert 2009). A sample clustered data can be shown in Figure 6, in which different color means different clusters.

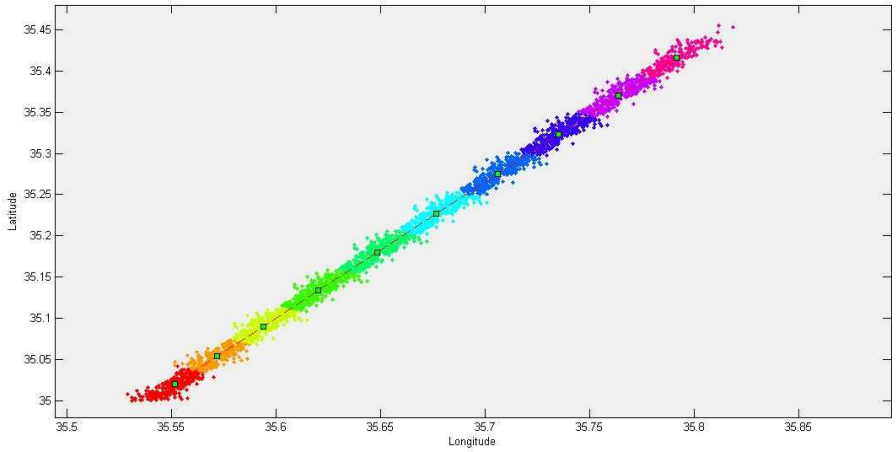

Figure 6 Pass 159 T/P, J-1 Clustering Sample

3.2 Statistical Tests on Data

To model and test data linear least square adjustment (LLSA) method has been used as solution method. LLSA fitting method has huge amount of place to adjust and model SSH data in different studies. LLSA is a kind of method to estimate unknown parameters given by minimizing the sum of the squares of residuals of the observations from estimated parameters' expected values. LLSA has major advantages to use distributed data in spatial and in time. These advantages can be listed as following (Koch 1999), (Pugh 1987).

- It does not depend on length of data
- Fitting procedure can be applied to data for any time span
- Data gaps do not limit the analysis
- No assumption is needed to perform fitting procedure

Least square estimation is used for the estimation of unknown parameters on the basis of Gauss Markof Model which is given by equation 3.1.

$$\boldsymbol{y_{nx1}} + \boldsymbol{e} = \boldsymbol{x_{nxu}\beta_{ux1}} \qquad \text{with } E(\boldsymbol{e}) = 0 \tag{3.1}$$

Hereby, n is number of observations, u is number of parameters, e israndom measurement error which makes the equation consistent, y represents observations, x is jacobian matrix. Note that measurements are accepted as equally weighted and uncorrelated so that **P = I.** The estimated parameters are obtained from equation 3.2.

$$\widehat{\boldsymbol{\beta}} = (\boldsymbol{X^T X})^{-1}\boldsymbol{X^T y} \tag{3.2}$$

The estimated residual is given in equation 3.3.

$$\hat{\boldsymbol{e}} = \hat{\boldsymbol{y}} - \boldsymbol{y} \tag{3.3}$$

Then, variance factor

$$\hat{\sigma}_0^2 = \frac{\hat{\boldsymbol{e}}^{\boldsymbol{T}}\hat{\boldsymbol{e}}}{n-u} \tag{3.4}$$

Variance covariance matrix of the observations

$$D(\boldsymbol{e}) = D(\boldsymbol{y}) = \sigma^2 P^{-1} \tag{3.5}$$

For the assessment of the result variance covariance matrix of parameters is also needed

$$\mathrm{D}(\widehat{\boldsymbol{\beta}}) = \hat{\sigma}_0^2(\boldsymbol{X^T X})^{-1} \tag{3.6}$$

Note that all these procedures have been made in every linear regression steps for both SSH data and SLH data.

To understand the statistical distribution of data set and statistical significance of model parameters, outlier detection and significance tests have been implemented in each clustered data. An outlier can be defined

as a value that is numerically distant from the other data (Barnett ve Lewis 1994), (Koch 1999). Standardized residual is

$$\bar{e}_{i,p}=\frac{|e_i|}{\hat{\sigma}_0\sqrt{Q_{e_ie_i}}} \tag{3.7}$$

Here,$\hat{\sigma}_0$ is given as apposterori variance, $\mathbf{Q_{ee}}$ is weight coefficient matrix of residuals, $\bar{e}_{i,p}$ is standardized residual. For the implementation of Pope Outlier test, tau distribution value is taken into account as table value. Outlier is detected with the following expression

$$\bar{e}_{max,p} > \tau_{f,1-\alpha_0/2} \tag{3.8}$$

To define the variation of observations with respect to time, second trend function of least square adjustment model is being used (Wolberg 2006). The statistical significance of trend parameters is tested based on Test t.

$$\boldsymbol{t} = \frac{\hat{\boldsymbol{\beta}}}{\hat{\boldsymbol{\sigma}}_{\hat{\boldsymbol{\beta}}}} \tag{3.9}$$

Herein, $\hat{\boldsymbol{\beta}}$ represents vector of parameters, $\hat{\boldsymbol{\sigma}}_{\hat{\boldsymbol{\beta}}}$ is standard deviation of parameters. T test accepts the parameters of trend function as significance values, if computed t value is bigger than table t value.

With the scope of this study, two outlier detection methods have been applied to the altimetry data. As mentioned above first one is Pope Outlier test, and the second one is Interquartile (IQR) outlier detection method.

IQR is based on median value of data. In IQR method, firstly the main median (Q2) of the all data must be computed. Then, the low median (Q1) and high median (Q3) are calculated. Q1 and Q3 are deduced from the data which are less and greater thanmain median value, respectively. Afterwards, the range (R) between the difference of Q1 and Q3 is computed (Upton ve Cook 1996). A measurement (M_i) is accepted as outlier, if

$$M_i > Q_3 + \left(\frac{3}{2}\right)R \quad \text{or} \quad M_i < Q_1 + \left(\frac{3}{2}\right)R \tag{3.10}$$

The results from IQR and Pope Test are checked out according to the statistical criterion called as percentage error band (PEB) which is explained in the next section.

3.3 Selecting Outlier Detection Method

Outliers detected by means of Pope Test and Interquartile are compared cluster by cluster for selecting the best method with the value of PEB. The PEB value is simple and useful method to be able to choose the proper outlier detection method. For each cluster the PEB value is calculated as follows (eHow 2011), (Tiwari, et al. 2007):

$$PEB = \frac{X_i - \bar{X}}{X_i} 100 \tag{3.11}$$

In here, X_i is observation detected as outlier within its own cluster, $\bar{X}$ is mean value of data in the cluster. The PEB values of detected outliers show difference in Pope Test and IQR. It is appropriate to have observations with the lower PEB value (Tiwari, et al. 2007), (Allison 1999).

Through PEB value approach, all data are examined by appropriate outlier detection method. Note that the lowest PEB value is 1.57, the greatest value is 9.34. It is resulted from PEB value approach that Pope Test is dominantly better than IQR for the case. Totally, in only one cluster Iqr method gave good result against with Pope. The number of appropriate results can be seen in Table3.

Table 3 Number of Clusters with Appropriate PEB Value

Pass Number	Number of Pope Dominated Clusters	Number of Iqr Dominated Clusters	Number of Clusters with Equal PEB Value	Number of Clusters with No Outlier Detected
68	24	-	-	7
159	8	-	-	2
170	18	1	1	15
246	14	-	3	11

3.4 Interpolation of SSH Data

After being progressed with respect to some statistical criterion like outlier detection and significance test of the model, each data is brought to the center of its cluster by means of geoid height extracted from Earth Gravitational Model 2008 (EGM08) (Pavlis, et al. 2008).

hsynth_WGS84.f program has been used to calculate geoid undulations from spherical harmonic synthesis of the EGM2008 Tide Free Spherical Harmonic Coefficients and its correction model (Zeta-to-N_to2160_egm2008). As input, user must give the latitude and longitude of points where geoid undulations needed to be computed. Thus the output includes latitude, longitude and geoid height of the points.

To process the interpolation procedure, geoid height is computed in every point of data and at the position of each cluster center. Thereafter, geoid height is used as slope surface with the linear calculation basis in the form of following solution

$$SSH_{cor} = SSH_i + (N_{ci} - N_i) \quad (3.12)$$

Here, SSH_i is the measured SSH of each point, N_i is the geoid height of each measured point position, $N_{ci}$is symbol to show the geoid heights of each cluster center. The maximum value ofdistancebetween measured

point position and the position of its cluster's center was approximately 4 km. To illustrate, a sample figure is given in Figure 7.

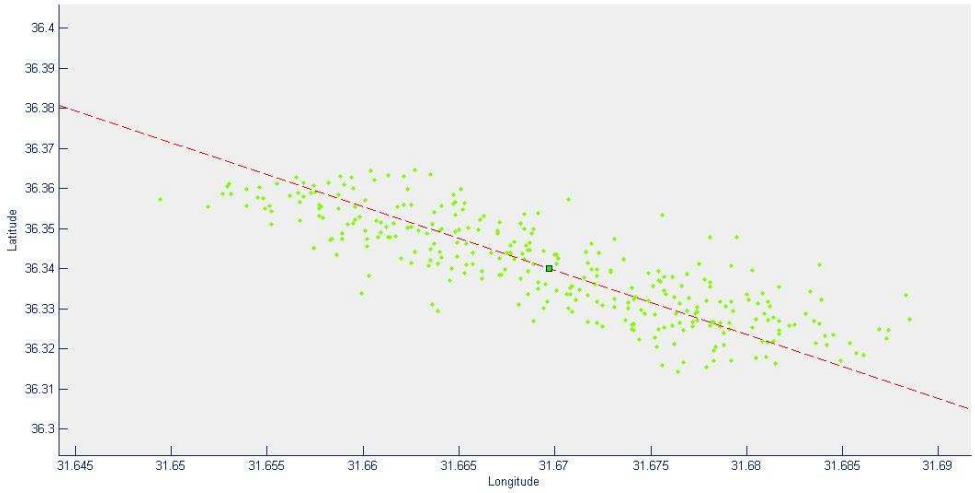

Figure 7 Each Measured SSH is brought to its Center

After bringing the observations to their centers standard deviations of clusters have been changed. This change is given in Table 4 for Pass 159.

Note that there is an enormous change of standard deviation in each clustered data set. To illustrate, for Pass 246, before centered mean of standard deviation is 0.1438 m., on the other hand, after centered standard deviation becomes0.0909m. It makes sense that using geoid height as slope surface is an applicable method on SSH relocation. All standard deviations of relocated SSHs are given in Appendices part of this study.

Table 4 Std. of SSH Observations Before and After Centered

Cluster Number	*Std. of SSHs Before Centered (cm)*	*Std. of SSHs After Centered (cm)*
1	11.16	7.88
2	11.07	8.12
3	10.84	8.33
4	11.42	8.17
5	11.71	8.10
6	12.42	8.62
7	12.19	8.65
8	12.50	8.91
9	11.92	8.52
10	12.51	9.17

Afterwards, to be able to analyze data spectrally whole data must be fulfilled with a proper method. In this study, PCA has been used to analyze clusters and their similarities, thus, each cluster has been fulfilled before PCA method is applied. With this aim, SSH values handled as a time series signal to analyze.

After analyzing SSH as a time series signal, data gaps are fulfilled by two kind of methods. This process has been performed based on time domain and frequency domain approach. For time domain approach cubic spline interpolation method has been run, on the other hand, for frequency domain one Lomb-Scargle algorithm has been used in this study. Due to becoming appropriate structure for unevenly spaced data, for time domain; cubic spline, and for frequency domain; Lomb-Scargle methods have been selected to implement in SSH time series.

3.5 Time Domain Interpolation of SSH Time Series

Since having gapped data in each cluster, SSH time series are analyzed in time domain and spectral domain. As time domain solution, cubic spline method has been chosen to interpolate SSH time series in each cluster. Cubic Spline interpolation works well in condition of existing gapped data (De Boor 2001).

As it is well known, a simple curve fit is based on one equation for all n points. However, a cubic spline allowing each segment to have a unique equation. In cubic spline, the routine fits n equations for n intervals subject to the boundary conditions of n+1 data points. The form for the cubic polynomial curve fit for each segment is given in equation 3.13.

$$\boldsymbol{y = a_i(x - x_i)^3 + b_i(x - x_i)^2 + c_i(x - x_i) + d_i} \qquad (3.13)$$

The routine must ensure that $y(x), y'(x) and\ y''(x)$ are equal at the interior points for adjacent segments. In this study, x values are considered as times, i is for gapped data, and y values are SSH observations. The cubic spline parameters a,b,c,and d are defined from known observations to interpolate data gaps at given time for each cluster.

The cubic spline is an easy to implement curve fit routine. Because the method includes connecting individual segments, so that the cubic spline avoids oscillation problems in the curve fit. After all, the cubic spline provides good curve fit for unevenly spaced data points (Lilley 2002), (O'Neill 2002).

A sample spline interpolation result is shown in Figure 8.

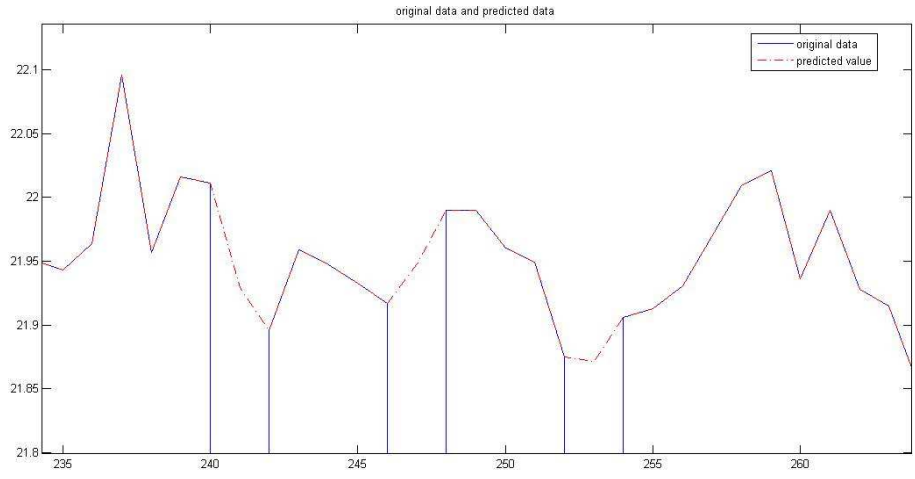

Figure 8 A Sample of Cubic Spline Interpolation, J1-T/P Pass159

While blue lines are for gapped data points, dashed red lines represent cubic spline interpolation predictions.

3.6 Spectral Analysis of SSH Data

Any periodical signal in the timedomain can be deduced from the sum of sine and cosine signals of different frequency and amplitude. This sum is called as Fourier series. Fourier series represent a wave that repeats itself. If the wave is complicated, it is the sum of simple waves (Rauscher, Janssen and Minihold 2001), (LEX 2006).

Fast Fourier Transform is the most popular technique to transform the signal into the frequency domain. However, if data have some gaps, some other techniques like Lomb Scargle or McClean may be used to analyze the data in frequency domain. Due to existing of gaps in data, Lomb scargle algorithm is handled in this study.

Lomb scargle is a method to predict a frequency power spectrum through a least squares fit of sinusoids to original data. This method is similar to Fourier analysis. But Fourier analysis gives power spectrum of signal with more noises than Lomb Scargle in the case of gapped data records (Ibanoglu 2000), (Birney, Gonzalez and Oesper 2006), (Press, et al. 2007).

The Lomb Scargle method is also known as least square spectral analysis. Simply, a periodogram is a prediction of spectral density of a signal.Lomb Scargle uses Lomb Scargle Periodogramand least-squares fitting of chosen frequencies of sinusoids computed from such periodograms (LombScargle tarih yok). The method evaluates data, and sines and cosines, only at times t_i that are actually measured with given freqencies ω_i ($2\Pi f_i$). Then, predicts amplitude coefficients A and B to find SSH where actual measurement has not gathered.

The lomb scargle can be presented as equation 3.15.

$$h_{ti} = A cos\omega_i t_i + B sin\omega_i t_i \qquad (3.15)$$

In this study, ω_i is input frequency coming from measurement times, h_{ti} is actual SSH data, A and B are coefficients of amplitude of signal deduced from SSH time series.

One step before using amplitudes which are found by lomb scargle method, there is a significance test must have been made on amplitudes for each SSH time series. According to significance level (α), significant amplitude and its frequency have been defined with alpha = 0.05 significance level. Also, the significant periods derived from significant frequencies are deviating from 1 to 8 years. For further information, all significant periods can be found at Appendices. It can be said that there are some local periodical effects on SSHs which may not be modeled by global ocean tide model (GOT 4.7). A sample resulting figure showing Lomb Scargle Power spectrum can be seen in Figure 9. It represents first cluster of Pass 159.

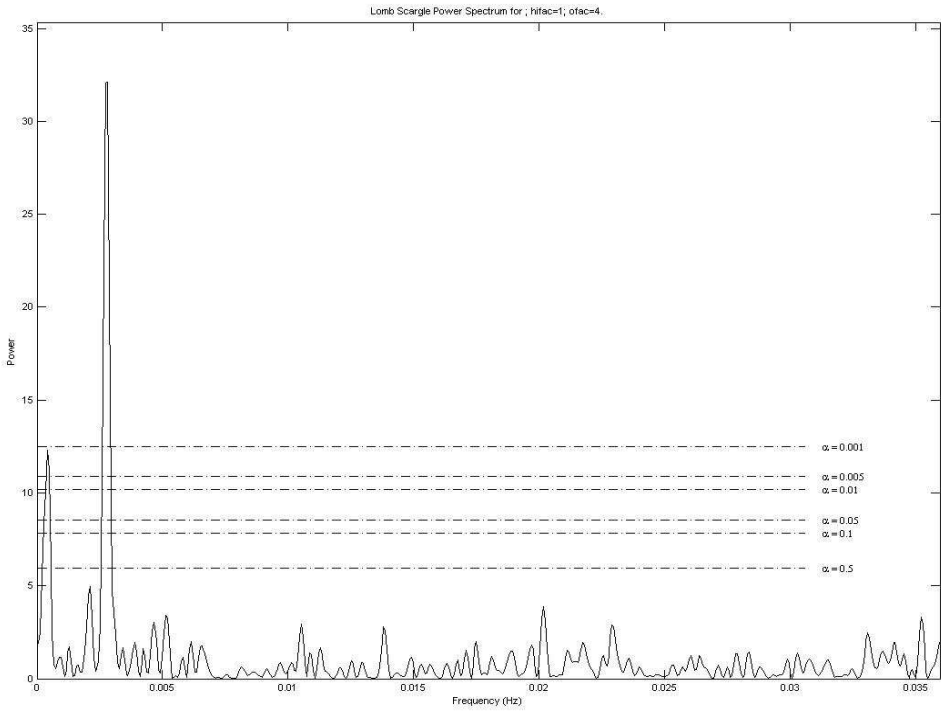

Figure 9 A Sample Lomb Power Spectrum for J1-T/P, Pass 159

After having interpolated SSH time series for gapped data times, a comparison has been made among the results between cubic spline interpolation and Lomb Scargle interpolation. As a general result, standard deviations of Lomb Scargle outputs were approxiametly 1.5 cm lower than cubic spline outputs. To illustrate, the standard deviation of spline interpolated data set for one cluster was ±8.39 cm, while the standard deviation of Lomb Scargle interpolated one was ±7.18 cm.Then, Lomb Scargle interpolation values are used in interpolation process for each data sets to perform PCA method. Details about standard deviations of Pass 159 for each cluster can be seen in Table 5.

Table 5 Comparison of Std. between Cubic Spline and Lomb Scargle

Pass No. 159	Std. from Cubic Spline (m)	Std. From Lomb Scargle (m)
1	0.0839	0.0718
2	0.0851	0.0706
3	0.0817	0.0782
4	0.0818	0.0796
5	0.0923	0.0787
6	0.0858	0.0841
7	0.0866	0.0850
8	0.0881	0.0875
9	0.0847	0.0829
10	0.1118	0.0804

3.7 Principle Component Analysis (PCA) on SSH

PCA is a way of describing patterns in data, and extracting remarks about similarities and differences of data. Since finding procedure of patterns is difficult to realize in high dimension data, PCA is a useful technique in order to analyze data. PCA is to re-expressing the data as a linear combination of its basis vectors as well. Also, data can be compressed by PCA with the help of reducing dimensions of it. This process does not lead to much loss of information. Generally PCA method progress composes of five major steps. These steps are

- subtract off the mean for each cluster,

- getting the covariance matrix,
- calculating the eigenvectors and eigenvalues of the covariance matrix,
- selecting components and forming a feature vector,
- deriving new data set.

Hereby, mean subtracted off time series of SSH values can be defined as matrix like

Time

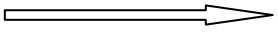

$$\boldsymbol{A} = \begin{bmatrix} A_1(1) & A_1(2) & A_1(3) & \dots & \dots & A_1(N) \\ A_2(1) & A_2(2) & A_2(3) & \dots & \dots & A_2(N) \\ \dots & \dots & \dots & \dots & \dots & \dots \\ A_m(1) & A_m(2) & A_m(3) & \dots & \dots & A_m(N) \end{bmatrix} \quad (3.16)$$

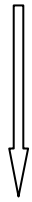

Space

The **A** matrix includes SSH values for m number clusters and n number measurements. The **A** matrix can be split into time and space orthogonal basis through covariance matrix. The covariance matrix can be represented like

$$C_A = (A * A^T)_{MxM} \quad (3.17)$$

Besides, matrix form of covariance value is

$$\boldsymbol{C_A} = \begin{bmatrix} V(A_1) & C(A_1A_2) & \dots & C(A_1A_M) \\ C(A_2A_1) & V(A_2) & \dots & C(A_2A_M) \\ \dots & \dots & \dots & \dots \\ C(A_mA_1) & C(A_MA_2) & \dots & V(A_M) \end{bmatrix} \quad (3.18)$$

Diagonal elements of $\boldsymbol{C_A}$ are the variances, and off diagonal elements are covariances as well. After setting up covariance matrix, eigenvalues and eigenvectors can be determined like

$$\boldsymbol{C_A} * \boldsymbol{K} = \boldsymbol{K} * \boldsymbol{\lambda} \quad (3.19)$$

This means that $\boldsymbol{C_A}$ matrix can be resolved to **K** and **λ** matrices, and can be represented by means of them. Here, **λ** is eigenvalue of $\boldsymbol{C_A}$, and in the matrix from:

$$\boldsymbol{\lambda} = \begin{bmatrix} \lambda_1 & 0 & \dots & 0 \\ 0 & \lambda_2 & \dots & 0 \\ \dots & \dots & \dots & \dots \\ 0 & 0 & \dots & \lambda_m \end{bmatrix} \tag{3.20}$$

Eigenvalues are in decreasing order, and all eigenvalues are equal or more than zero. On the left side, **K** is the eigenvector of cov_{AA} matrix. Additionally, **K** is the square matrix and has MxM dimensions corresponding related **λ** value..

$$\boldsymbol{K} = \begin{bmatrix} K_1^1 & K_1^2 & \dots & K_1^M \\ K_2^1 & K_2^2 & \dots & K_2^M \\ \dots & \dots & \dots & \dots \\ K_M^1 & K_M^2 & \dots & K_M^M \end{bmatrix} \tag{3.21}$$

⇩ Eigenvectors

Let **I** is the identity matrix, **K** eigenvectors matrix has feature that

$$\boldsymbol{KxK^T} = \boldsymbol{K^TxK} = \boldsymbol{I} \tag{3.22}$$

This means that eigenvectors are uncorrelated, namely, orthogonal to each other. Then the principal components **(F)** can be deduced from

$$\boldsymbol{F} = \boldsymbol{K^T} * \boldsymbol{A} \tag{3.23}$$

Any λ eigenvalue in relation with considered **A** matrix value. Then, it can be computed like following part:

$$\% \text{ Variance mod} = \frac{\lambda_i}{\sum_{t=1}^{i} \lambda_t} * 100 \tag{3.24}$$

In this study, as explained above, association behavior is derived from this variance percentage.

Note that the covariance shows the degree of the relationship between variables. A high positive value indicates positively correlated data. Eigenvectors are also known as characteristic vectors, and the eigenvalues can be called as characteristic values of considered data set. Eigenvectors are perpendicular to each other meaning that they are uncorrelated (Smith 2002), (Shlens 2009), (H. Yıldız 2005), (Govaert 2009).This means that high level correlation between data sets results in high eigenvalue of considered data sets. Similarity percentage of signals has been calculated from ratio that eigenvalue of a signal to sum of eigenvalues of all signals in that group.The eigenvalues indicate how much variance is explained by each eigenvector.

In this study, PCA procedure is run to extract behavior of each cluster with respect to the otherclusters.Note that the altimetry Passes are numbered in clusters according to their latitude. This means the higher number of cluster, the closer point to tide gauge station. To illustrate, for Pass 159, 10 clusters have been created, and 10^{th} one is the closest cluster to İskenderun Tide Gauge.

In this study, clusters are handled as a group of five clusters in PCA analysis. To represent the details, Table 6 is generated below.

Table 6 PCA results for Pass 159

Pass	***Clusters***	***Percentage***
159	06 - 10	76.28
	05 - 09	83.44
	04 – 08	84.60
	03 – 07	81.06
	02 – 06	73.53
	01 - 05	65.51

Herein, percentage values denote that first principal component derived from considered group of clusters represents variability of SSH with the value in percentage column. For example, the 84.60 is the value of first

principal component to represent behavior of the group covers from 4 to 8 clusters. Figure 10 is to explain this aspect.

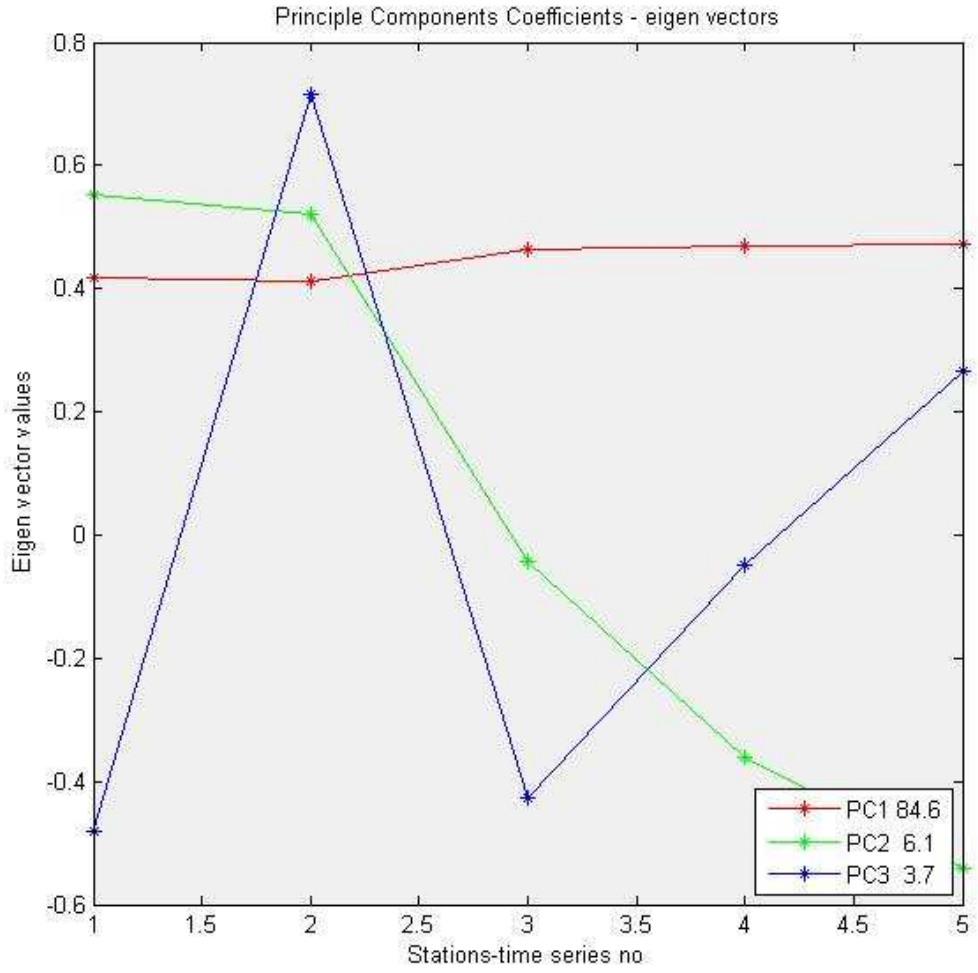

Figure 10 Leading Three Spatial Models of Variability (eigenvectors)(Clusters 4-8)

It is seen in Figure 10 that if the clusters between 4 and 8 are chosen first principal component can explainthe variance in the original data set with 84.6% percentage. Only 5th cluster disturbs the harmony of these clusters. On the other hand, looking at Principal components of all clusters can make sense to figure out Figure 10 well through Figure 11.

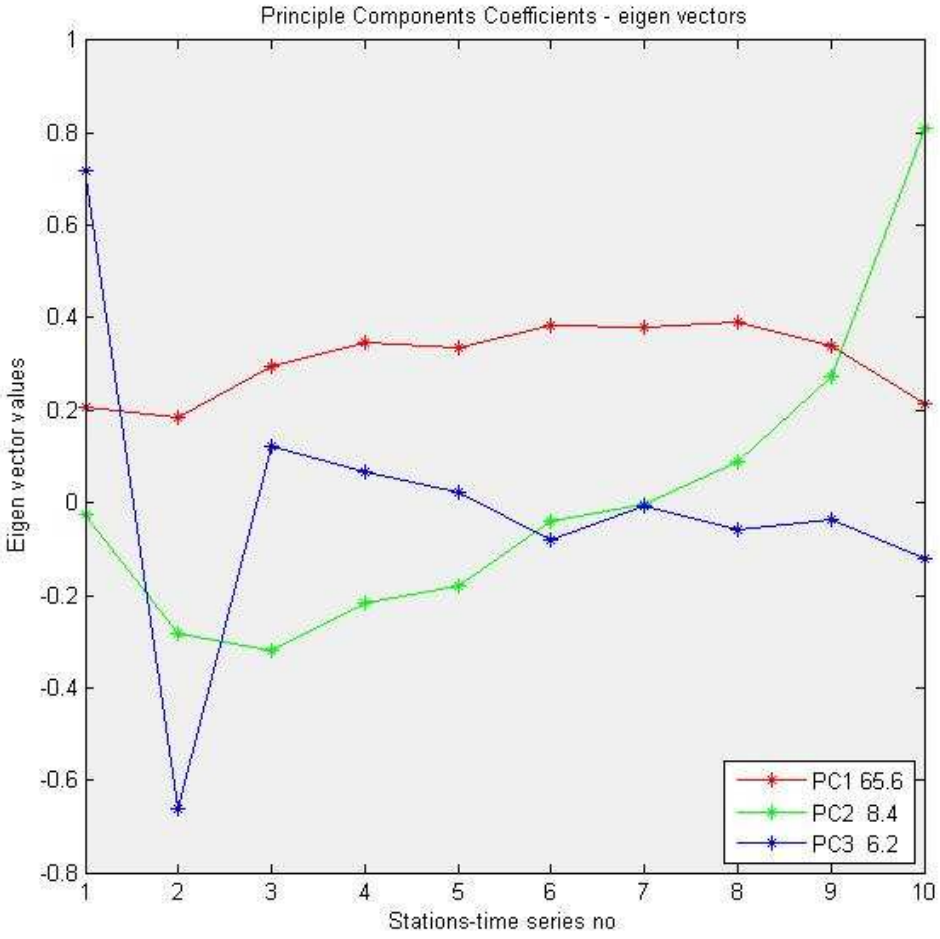

Figure 11 Leading Three Spatial Models of Variability (eigenvectors)(All Clusters)

It is easily recognized that first principal component is being disturbed especially by 2nd, 5th and 10th clusters, and represent variance only with 65.6 %. Thus, this approach can be applied to all Passes which are clustered like in this study. The main three principal components derived from 4 to 8 clusters can be seen in Figure 12.

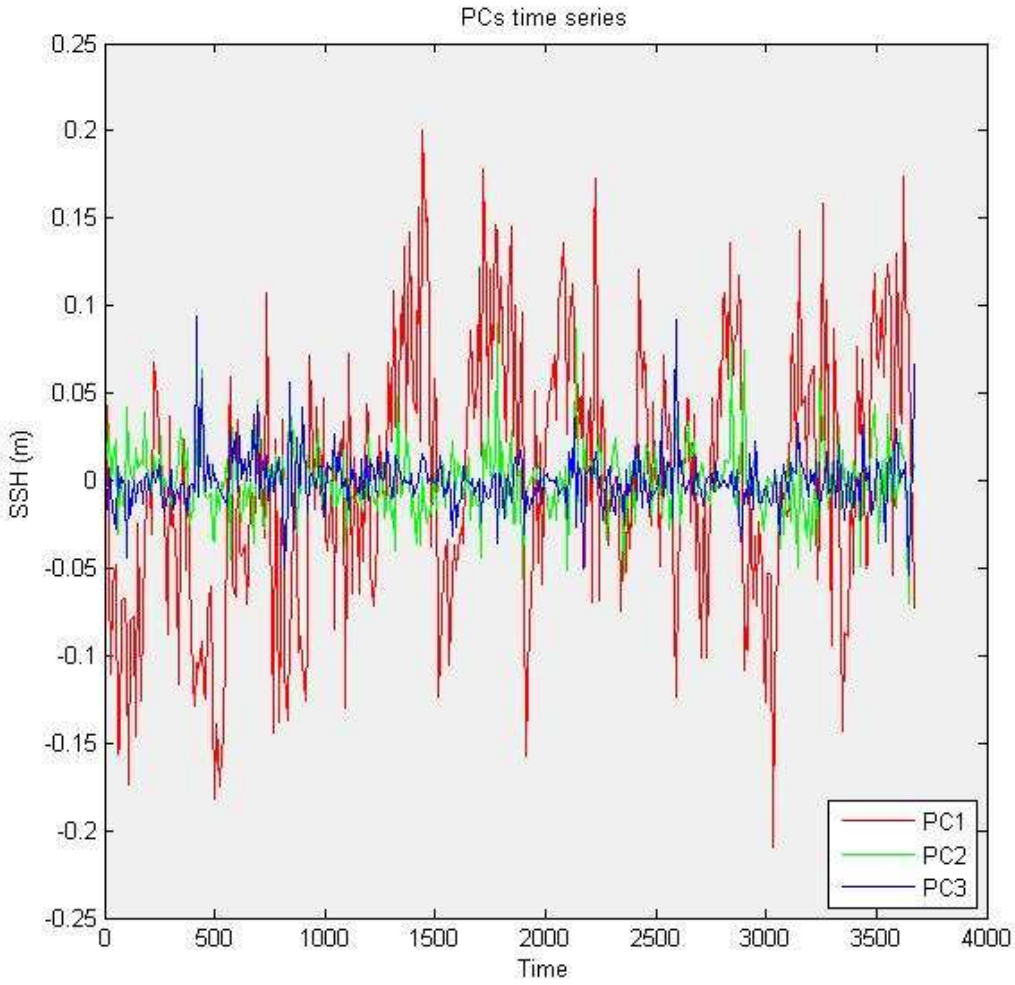

Figure 12 Leading Three Principal Components (temporal modes of variability)

Since grouping has been started at closer point to coast line, similarity percentage generally becomes low in four different passes in this study. It would be better to investigate in relation of similarity percentage and bathymetry data, however, as it is mentioned in many studies signals have been distributed due to mainly shallow water affects, sea waves and lack of global model for coastal zones. For all used Passes in this study, similarities near with coasts and best similarities are given with their cluster numbers in Table 7.Consider the fact that these values are deduced from the first principal component of cluster groups.

Table 7 Most Similar and Coast Cluster Data Groups

Pass Number	*Clusters*	*Percentage*
68 (at the coast)	27 - 31	65.88
68 (most similar)	03 – 07	86.61
159 (at the coast)	06 - 10	76.28
159 (most similar)	04 - 08	84.60
170 (at the coast)	31 – 35	65.27
170 (most similar)	03 – 07	90.28
246 (at the coast)	24 – 28	69.66
246 (most similar)	04 – 08	86.60

According to similarity percentage, a group of five clusters has been chosen to extract SSH trends from the most similar one group clusters.

Herein, only the trends of Pass 159 are given to see SSH trends and similarity percentage together. Through Chapter 5, SSH trends from altimetry missions and SLH trends from tide gauges will be investigated in detail. To illustrate, the figure of Pass 159 clusters is shown in Figure 13. Note that clusters which are used to extract SSH trend are rounded with red circle in the figure below.

Figure 13 All Clusters of Pass 159

SSH linear trends are deduced from regression analysis of SSH data sets in each cluster. Significance test of trend parameters and SSH trends can be seen in Table 8.To sum up, the SSH trends of each Pass are arithmetic mean of chosen clusters.

Table 8 SSH Trends and Test Values of Pass 159

Cluster Number	***SSH Trend (mm)***	***STD. of Trend Parameter (mm)***	***T Test Value (must be >1.28)***
1	+ 2.3	± 1.3	1.77
2	+ 4.4	± 1.3	3.45
3	+ 6.8	± 1.4	3.80
4	***+ 8.4***	***± 1.4***	***4.84***
5	***+ 7.2***	***± 1.4***	***5.22***
6	***+ 9.2***	***± 1.4***	***6.32***
7	***+ 8.8***	***± 1.5***	***5.94***
8	***+ 8.1***	***± 1.5***	***5.30***
9	*+ 6.0*	*± 1.5*	*4.05*
10	+ 2.4	± 1.5	1.66

As it is seen in Table 8, from the similarity percentage of PCA method, the clusters from 4 to 8 (bold in table 8) are used in extracting trends of SSH to compare with İskenderun Tide Gauge SLH trend. Thus, SSH trend is found as +8.02 mm/yr with ±1.5 standard deviation for Pass 159 from Jason-1 and T/P data set. Also, trend value definedwith linear regression from first principal component of chosen group is +8.04 ±1.3 mm/yr.

Since further results and comments will be mentioned in Chapter 5, only for Pass 159 altimetry trends are given in this Chapter. To analyze SLH from tide gauge observations, brief information about tide gauges and analysis methods are emphasized in the next chapter. Then, daily and monthly MSLs are computed for seeing SLH trends in Antalya, Bodrum, Erdemli and İskenderun Tide Gauges.

Note that all other Passes have been processed with the same procedure. The results of each passes can be seen in appendices part of this study.

CHAPTER 4

TIDE GAUGE DATA and PROCEDURE

4.1 Introduction

Sea level variation has been observed by means of tide gauge measurements gathered over the last century.A tide gauge is aninstrument for measuring sea levelrelative to the ground. Tide gauges may also move vertically with the region as a result of post-glacial rebound, tectonic uplift or crustal motion. This enormously sophisticates the matter of describing SLHvariationfromtide gauge data. GPS obtains absolute verticaltrend information so that the sea level data of tide gauges can be defined at the same reference system with satellite altimetry, then it is possible to compare tide gauge and altimetry data directly (IOC 2000).

Differences in SLH estimates from tide gauge data express the need to account for vertical crustal movements. Tide gauges are exposed tometeorological influences acting on SLHs like barometric pressure and wind speed. These variables can be removed from long-term evaluations of SLH change (Colorado University SLR 2011). Not only tide gauge data has been used in definition of ocean currents, but also it has been very useful tool to define long term sea level changes. Specifically, tide gauge data are in service to describe vertical datum and vertical crustal motion as an application of geodesy (Yıldız, et al. 2003). A schematic represent

of tide gauge is given in Figure 14 (Colorado University SLR 2011), (JCOMM 2006).

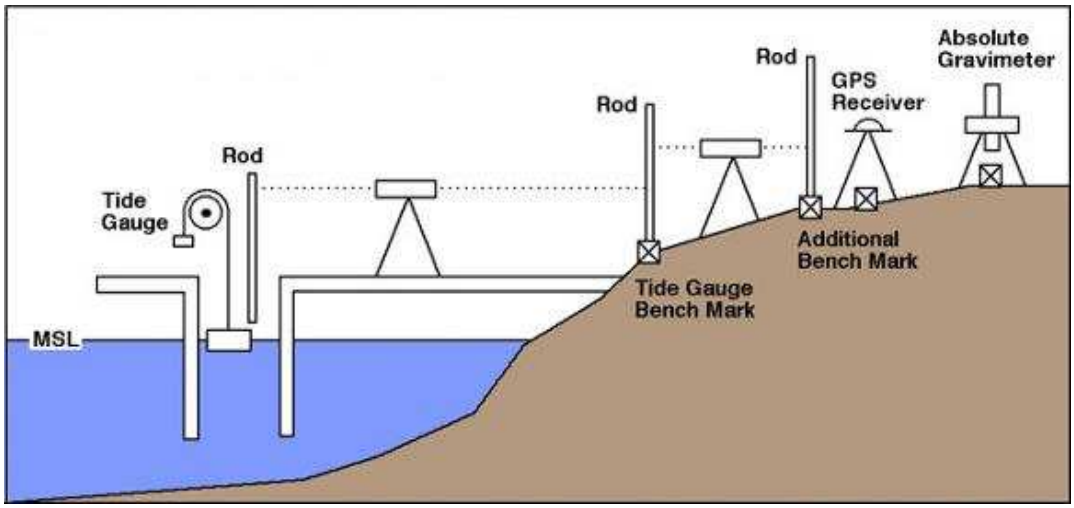

Figure 14 A Tide Gauge Measurement System (Colorado University SLR 2011)

The tide gauge data must be carefully calibrated, checked and evaluated. The measurements should be connected to local benchmarks which are fixed into national leveling network and then fixed into the global network by means of modern geodetic techniques. The recorded data need to be archived, documented and protected for future studies. Afterwards data can be considered as a valuable resource and can be used for studies ranging from local engineering projects to long-term global climate change (JCOMM 2006). Tide gauges can be split into three parts according to measurement instrument. These are acoustic gauges with sounding tubes, pressure sensor tide gauges and stilling well gauges. Acoustic gauges with sounding tubes form the basis of Turkish Sea Level Monitoring Network (H. Yıldız 2001).

4.2 Products of A Tide Gauge

Sea level variations can be measured by tide gauge data. These measurements are in service in a wide range of application areas which

aredetailed in following table, Table 9 (Yıldız, et al. 2003), (Carrera and Vanicek 1985), (ESEAS 2001).

Table 9 Application Areas of Tide Gauge Data (Yıldız, et al. 2003)

Application Area	Explanations
Geodesy	• Definition of vertical datum • Enhancing the precision of vertical control network • Control of geoid to define gravity • Definition of vertical land motion • Definition of post-seismic and Pre-seismic activities
Oceanography, Climatology, Geophysics, Geology, Meteorology	• Definition of sea slope for estimation of ocean circulation • Calibration of satellite altimetry measurements • Geological researches • Climate change
Water Resource Management	• Input to define mixture of fresh water and sea water
Hydrology, Hydrography	• Correction of lead measurements • Definition of subsidence transfer roads • Harbor design
Shipping	• Sea Navigation • Guidance of shipping
Human and Environmental Security, Saving Coastal Areas	• Warning and prediction of storms • Design of protection set

The effects causing the variation of sea level variations are meteorological effects, oceanographic effects, tides, climate change and vertical crustal motion.

At the level of preprocessing of tide gauge data, some software can be used to tie sea level measurements to a reference point, detection of time and datum bias with the aid of graphical support, fulfill the short

gaps. There are three generally known software to use sea level measurements properly; SLPRC, TASK and FIAMS. These tools utilize to predict tide analysis, realize quality control and perform filtering (Yıldız, et al. 2003).

4.3 Tide Gauge Data

In this study, four tide gauges hourly data have been used to analyze sea level trends. These tide gauges are Antalya, Bodrum, Erdemli, İskenderun. The detailed information about time interval and geodetic coordinates are shown in Table 10.

Table 10 Used Tide Gauge Data

Station Name	Time Interval (hourly)	Position (lat,lon)
Antalya	2003.1-2010.12	36.8285,30.6093
Bodrum	2003.1-2010.12	37.0323,27.4235
Erdemli	2003.5-2010.12	36.5634,34.2550
İskenderun	2004.12-2010.12	36.5932,36.1802

Not only all hourly data have been given with outlier detected, but also all error sources were classified by data service provider, GCM. To illustrate, a sample of obtained data format is shown in Figure 15.

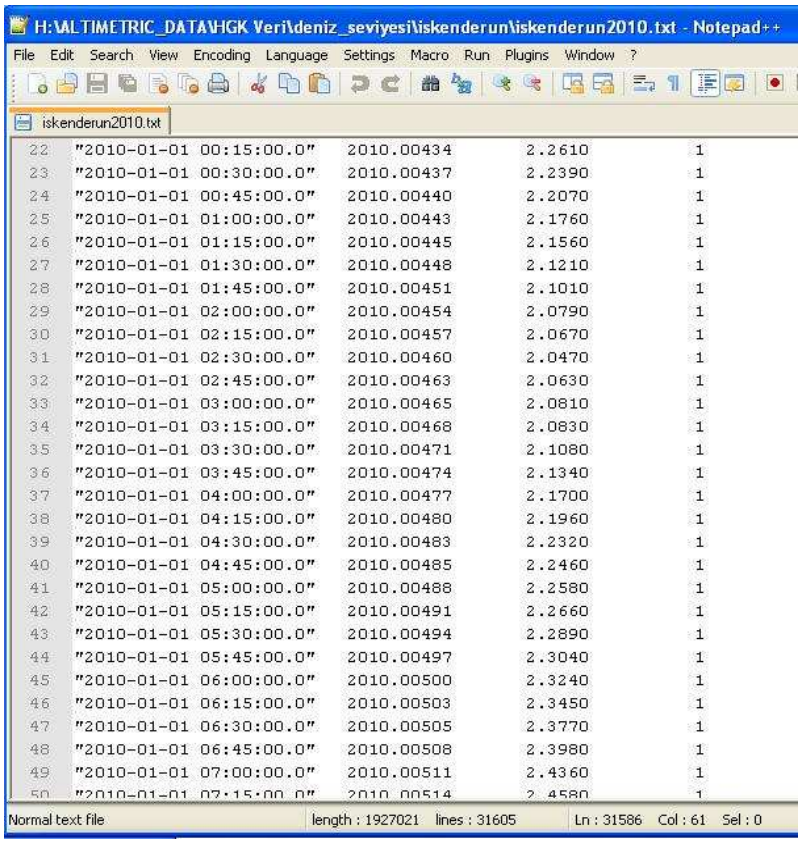

Figure 15 A Sample of Hourly TG Data Format

First column shows Date and Time of observation, second column is its decimal year, third column is for SLH observation at that time, and fourth one is to give error classification value, data flag. Data Flag number changes in range from 0 to 9. Zero data flag value means that no quality control has been made on that value, 1 is for correct value. See the Table 11 for all data flag numbers and their meanings.

Table 11 Hourly Data Flags for Error Classification

Data Flag Value	*Explanation of Data Flag Value*
0	No quality control
1	Correct value
2	Interpolated value
3	Doubtful value
4	Isolated spike or wrong value
5	Correct but extreme value
6	Reference change detected
7	Constant values for more than a defined time interval
8	Out of range
9	Missing value

Due to already having classified data on the basis of outlier detection, the next step, a classical harmonic analysis of hourly data process has been performed on data.

4.4 Harmonic Analysis on Tide Gauge Data

As mentioned in Introduction Chapter, There are five main factors affecting on sea level heights like meteorological surges, oceanographic effects, tidal effects, climate changing, vertical crustal motion. To figure out periodical tidal effects on sea level heights in each tide gauges, tidal constituents must have been defined for these four tide gauges. After giving general information, used tidal harmonic analysis has been explained below.

Tides are the periodic sea level variations existing due to the combined effects of the gravitational forces.These forces exist mainly due to the moon, the sun and the rotation of the Earth. To observe the tide, the height of sea level is measured as a function of time with respect to a reference level. The tidal heights and characteristics change with their location and meteorological conditions. The range of a tide can vary from ten meters to a few milimeters (Chen and Lee 2001).

Some places on the open sea are exposed to two high and two low tides each day,semi-diurnal tide, but some locations are only one high and one

low tide each day, diurnal tide. The times and amplitude of the tides at the coast are affected by the incursion of the sun and moon, by the shape of the coastline and by the sample of tides in the deep ocean and at near coast bathymetry (Reddy and Affholder 2002), (Hubbard 1997).

Tidal changes are the result of some periodical influences acting in different frequencies and amplitudes. These influences are known as tidal constituents. The main constituents are due to the Earth's rotation, the positions of moon and the sun with respect to Earth, altitude of the moon above the Earth's equator, and bathymetry. Indeed, tidal forces act on whole Earth greatly, however, movement of the Earth is only in centimeters because of solid structure of the Earth.

Since tidal consituents on each tide gauges have different kind of periods and amplitudes, tidal analysis must be done for each tide gauges seperately. After performing tidal analysis, predicted signal can be used in fulfilling gapped data for desired epoch. Primary tidal constituents are given in Table 12.

Table 12 Primary Tidal Constituents

Tidal Component	*Period (Solar Hours)*	*Description*	*Nature*
M2	12.42	Principal Lunar	Semi-diurnal
S2	12.00	Principal Solar	Semi-diurnal
N2	12.66	Large Lunar Elliptic	Semi-diurnal
K2	11.97	Luni-solar	Semi-diurnal
K1	23.93	Luni-solar Diurnal	Diurnal
O1	25.82	Principal Lunar Diurnal	Diurnal
P1	24.07	Principal Solar Diurnal	Diurnal
Q1	26.87	Large Lunar Elliptic	Diurnal
MF	327.90	Lunar Fortnightly	Long term
MM	661.30	Lunar Monthly	Long term
SSA	4383.00	Solar Semi Annual	Long term

Tide gauges hourly data for each station have been analyzed for fulfilling data gap, and also for extracting tidal constituents. For this process, a classical tidal harmonic analysis approach has been implemented in hourly data. To perform tidal harmonic analysis, the classical tidal harmonic analysis including error estimates has been used by means of T_Tide.m program in MatLab (Pawlowicz, Beardsley and Lentz 2002).

The function of harmonic analysis is:

$$\boldsymbol{x(t)} = b_0 + \boldsymbol{b_1 t} + \sum_{k=1\ldots N} \boldsymbol{A_k \cos(\sigma_k) + B_k \sin(\sigma_k)} \quad (4.1)$$

Herein, t is measurement time, x(t) is hourly sea level of timet^{th}, b_0 is mean sea level at first epoch, b_1 is yearly mean sea level trend, N is the number of tide constituents, σ_k is frequency of tidal constituent, $A_k$and B_k are the coefficients of tidal constituent's amplitude. Thus, with the known frequency, the amplitude of tide gauge can be calculated from equation 4.2.

$$\boldsymbol{H_t} = \sqrt{\boldsymbol{A_k}^2 + \boldsymbol{B_k}^2} \qquad (4.2)$$

and phase angle from

$$g_t = arctan\ \frac{B_k}{A_k} \qquad (4.3).$$

By means of tidal analysis method, tidal constituents are extracted for each station, note that t is for considered tidal consituent number. Then, significance amplitudes have been defined with respect to Signal-to-noise ratio (SNR) value. Tidal constituents which have SNR value greater than 2, is taken into account to get predicted signal for each station.

SNR is defined as the ratio of signal power to the noise power. It is seen that if SNR value is equal or bigger than 2predicted values are consistent to each other. This fact results from comparison of parametric bootstrap and SNR.It is suggested that if a tidal constituent has lower than 2 SNR value, the tidal constituent should not be performed in the process of getting predicted value (Pawlowicz, Beardsley and Lentz 2002).

Significant tidal constituents and their SNR values for Erdemli station (2003-2010) are shown in Table 13.

Table 13 Significant Tidal Constituents of Erdemli Station (2003-2010)

Tide	*Frequency (1/hour)*	*Amplitude (m)*	*Amp. Error(m)*	*Phase (deg)*	*Phase Error (deg)*	*SNR*
SA	0.0001141	0.1057	0.013	229.95	6.64	65
SSA	0.0002282	0.0303	0.012	261.16	23.29	6.5
Q1	0.0372185	0.0028	0.001	242.40	10.19	30
O1	0.0387307	0.0193	0.000	256.08	1.35	1.7e+003
NO1	0.0402686	0.0013	0.000	253.20	18.01	12
PI1	0.0414385	0.0011	0.001	233.46	30.83	3.5
P1	0.0415526	0.0099	0.001	284.79	3.89	2.8e+002
S1	0.0416667	0.0086	0.001	246.71	5.05	1.1e+002
K1	0.0417807	0.0273	0.001	277.57	1.12	2.6e+003
PSI1	0.0418948	0.0015	0.001	173.71	22.40	6.9
J1	0.0432929	0.0014	0.001	266.67	21.70	6.9
OO1	0.0448308	0.0009	0.000	245.34	16.94	9.3
N2	0.0789992	0.0178	0.002	230.21	6.98	77
NU2	0.0792016	0.0032	0.002	228.32	37.53	2.4
H1	0.0803973	0.0047	0.002	302.05	24.52	4.9
M2	0.0805114	0.1068	0.002	228.97	1.18	2.2e+003
H2	0.0806255	0.0058	0.002	142.89	19.23	8.4
L2	0.0820236	0.0054	0.003	212.41	29.56	3.9
T2	0.0832193	0.0036	0.002	203.91	31.62	3.3
S2	0.0833333	0.0615	0.002	244.00	1.99	9.7e+002
K2	0.0835615	0.0172	0.001	241.72	5.30	1.4e+002
MSN2	0.0848455	0.0004	0.002	48.95	189.19	0.062
MO3	0.1192421	0.0007	0.000	33.13	19.73	11
M3	0.1207671	0.0026	0.000	1.44	5.15	1.1e+002
SO3	0.1220640	0.0003	0.000	84.46	48.86	1.7
MK3	0.1222921	0.0001	0.000	28.12	80.03	0.57
SK3	0.1251141	0.0010	0.000	294.90	12.84	21
M4	0.1610228	0.0007	0.000	292.94	12.99	28
MS4	0.1638447	0.0005	0.000	325.36	18.01	13
MK4	0.1640729	0.0002	0.000	325.40	30.87	4.4
2SK5	0.2084474	0.0001	0.000	282.55	40.98	2.2

Standard deviation of difference between input hourly data and hourly data obtained from predicted signal is ±9.10 cm for Erdemli Station. See relevant standard deviations for all stations used in this study in Table 14.

Table 14 Standard Deviation of Difference in Original & Predicted Data

Tide Gauge Station	*Time Span*	*Standard Deviation (cm)*
Antalya	2003.1-2010.12	±8.96
Bodrum	2003.1-2010.12	±8.29
Erdemli	2003.5-2010.12	±9.10
İskenderun	2004.12-2010.12	±10.37

To define tidal constituents more conveniently, there must be hourly tide gauge data for 18.6 years. Because, the significant tidal constituent which has the longest term period covers 18.6 years (H. Yıldız 2001). In this study, because of having less time span to seperate tidal constituents in each station, some long term tidal constituents have not been defined in data set (Yıldız, et al. 2003). Then, as it can be seen from the Table 13, standard deviation of difference between actual data and predicted data becomes lower rationally with measurement time span. Note that standard deviation occurs due to huge data gaps in actual data as well.

After extracting tidal constituents and getting predicted signal in each station for data gaps, filtering operation has been made to see daily and monthly mean sea level of each station.

4.5 Filtering of Hourly Data

As mentioned above, filtering is required to define mean sea levels firstly on the basis of daily, and secondly on the basis of monthly. SLPR2 program which is developed by cooperatin of University of Hawaii The Tropical Ocean Global Atmosphere Program Sea Level Center and the USA National Oceanographic Data Center has been used to calculate mean sea levels (TOGA tarih yok).

Program provides daily values from hourly data in two steps:

- Diurnal and Semi-diurnal components are removed
- To remove remaining high frequency, a 119-point low pass filter is applied.

Note that daily mean sea level can be calculated if there is a data gap less than 24 hours in hourly data. Outputs of predicted signal can be used to fulfill these considered data gaps. Therefore, monthly mean sea level data has been calculated from simple arithmetic mean of daily mean sea level. Also, if there is a gap of daily mean sea level data set covering more than seven days, related monthly mean sea level has not been calculated (Yıldız, et al. 2003).

In this aspect, filtering application has been made for all stations. Then, monthly mean sea levels have been compared with PSMSL monthly sea levels. It is seen that monthly mean sea level extracted from SLPR2 software by means of filtering hourly data was consistent with PSMSL monthly mean sea level data. Also, some data gaps existing in PSMSL data set has been fulfilled from calculated data set. Note that Table 15 includes PSMSL monthly mean sea level and calculated mean sea level between at the year 2009for Erdemli tide gauge.

Table 15 Calculated & PSMSL MSL for Erdemli, 2009

Month	Calculated Monthly MSL (m)	MSL from PSMSL (m)
1	1.008	1.008
2	1.181	1.181
3	1.096	1.095
4	1.086	1.084
5	1.105	1.105
6	1.214	1.214
7	1.306	1.306
8	1.275	1.275
9	1.256	1.257
10	1.203	1.203
11	1.233	1.233
12	1.306	1.306

It is mentioned that for data gap first of all the difference between predicted values and calculated values have to be computed. Then, for a gapped data time, the closest data must have been defined to apply linear interpolation for gapped time. Lastly, linear interpolation value must be added to predicted value. Note that this method is valid for less than 24 hour data gaps. Due to data consistency of MSL between PSMSL data and calculated data, predicted hourly values have been used directly to fulfill PSMSL data gaps in this study. Additionally, because of consistency between calculated and provided by PSMSL data set, PSMSL monthly mean sea level values have been used to extent monthly mean sea level data set. So that it is made possible using PSMSL MSL data set to see the SLH trends of each station.

Note that data gaps included in PSMSL data set has been fulfilled by calculated MSL values. To illustrate, PSMSL data set Antalya 2006 has no value in any month, but all the values of considered month are calculated by means of predicted values. Results can be seen in Table 16. The value of '9999' means that there is no MSL value for relevant month.

Table 16 MSL Values for Antalya 2006

Months for Antalya 2006	Calculated MSL values (m)	MSL values from PSMSL (m)
1	1.337	9999
2	1.302	9999
3	1.274	9999
4	1.272	9999
5	1.319	9999
6	1.395	9999
7	1.457	9999
8	1.471	9999
9	1.442	9999
10	1.400	9999
11	1.374	9999
12	1.310	9999

Moreover, PSMSL data set is extended for the year of 2010 obtained from hourly data for each station. For the year of 2010, calculated monthly mean sea level values are given in Table 16. Note that before adding these values to Antalya tide gauge MSL the yearly trend is calculated as +6.8, and after fulfilling with calculated MSL the yearly trends is +6.9 mm/yr. It is assumed that this process which is based on direct contribution of predicted hourly data is consistent to see yearly MSL height trends for this data set.

Table 16 Monthly MSL Values, 2010

Tide Gauge	*Month*	*Calculated Monthly MSL (m)*
Antalya	1	1.473
	2	1.460
	3	1.352
	4	1.292
	5	1.365
	6	1.468
	7	1.479
	8	1.537
	9	1.523
	10	1.440
	11	1.458
	12	1.528
Bodrum	1	1.327
	2	1.330
	3	1.342
	4	1.272
	5	1.329
	6	1.420
	7	1.396
	8	1.450
	9	1.453
	10	1.427
	11	1.449
	12	1.512
Erdemli	1	1.256
	2	1.221
	3	1.146
	4	1.086
	5	1.164
	6	1.277
	7	1.284
	8	1.326
	9	1.327
	10	1.240
	11	1.232
	12	1.325
İskenderun	1	2.269
	2	2.245
	3	2.180
	4	2.190
	5	2.220
	6	9999
	7	9999
	8	9999
	9	2.372
	10	2.288
	11	2.274
	12	2.303

Since the provided data has not measurement epoch at the months properly, sixth, seventh,eigth MSL values of İskenderun for 2010 have not MSL value. If measurement epochs would have been entered even with NaN (Not-a-Number) value, prediction values of these three months would be calculated.

Before getting through determining vertical trends chapter, processes can be summarized until this point. Firstly satellite altimetry measurements are clustered, detected against with outlier, trend parameters are tested, outlier methods have been compared, data gaps have been fulfilled on the basis of time and frequency domain. Then, PCA analysis has been run to see the similarity and differences in each cluster for used passes.

On the other hand, hourly tide gauge data was detected for outlier by data provider, GCM. Then, to define tidal constituents and fulfill data gaps of hourly sea level data, harmonic analysis has been made for each station. Therefore, It is possible to calculate daily and monthly MSL for each station.

To get more confident vertical trends from comparison of tide gauge and altimetry data, Global Positioning System (GPS) trends must be taken into account. However, as will be mentioned at the next chapter, there are some drawbacks to use GPS observations confidently.

CHAPTER 5

DETERMINING VERTICAL TRENDS

This chapter basically covers the trends of SSH from satellite altimetry and SLH from tide gauge observations. Although GPS trends are given by data provider, GCM, GPS campaigns cause some drawbacks to see vertical motion of crust directly. Therefore, GPS measurement epochs will be handled with explanations on the evaluating process of vertical motions.

5.1 Trends From Tide Gauges and Altimetry Satellites

As mentioned at the beginning, SLH trends deduced from tide gauges, mixed with crustal motion. Thus, it is needed to seperate this mix by means of external absolute observations like SSH derived from satellite altimetry.

To define the trends of tide gauges harmonic analysis has been applied to monthly MSL of each tide gauges. This harmonic analysis can be represented as

$$\boldsymbol{y_i} = A_0 + \sum_{j=1}^{M} \boldsymbol{A_j} \cos(\boldsymbol{w_j t_i} - \boldsymbol{\emptyset_j}) \qquad (5.1)$$

M constituents to be included in the analysis. As unknowns A_j and$\emptyset_j$are amplitude and phase of constituent, $w_j$is frequencyof constituent, y_i is the measured SLH,A_0 is averagesea level trend, i is the observation time, j is the number of constituents.

Also, frequencies as an input parameter can be seen in Table 17.

Table 17 Used frequencies for SLH Trends

Frequency Number	*Frequency (1/month)*	*Period (Month)*
1	0.0089559	111.6582
2	0.0233175	42.8862
3	0.0739339	13.5256
4	0.0788574	12.6811
5	0.0833281	12.0008
6	0.0878061	11.3887
7	0.1433533	6.9758
8	0.1478313	6.7645
9	0.1572547	6.3591
10	0.1666709	5.9998
11	0.1711489	5.8429
12	0.1756268	5.6939
13	0.249999	4.0000
14	0.254477	3.9296
15	0.3333344	3.0000
16	0.8689882	1.1508
17	0.8734662	1.1449
18	0.929006	1.0764
19	0.9334768	1.0713
20	0.9473782	1.0555
21	0.9523163	1.0501
22	0.9567943	1.0452
23	0.9612723	1.0403

In the process of defining SLH trends, significance of trend parameters has been tested with T test value. A frequency which has been found insignificant according to trend parameters, has been removed from input folder. Then, harmonic analysis has been started to be calculated from scratch. This process has been continued till finding at least one parameter of each retained constituent significant.

Moreover, linear regression analysis has been applied to the monthly MSL of each tide gauges. Trends computed from linear regression analysis and harmonic analysis are shown in Table 18.

Table 18 SLH Trends from Tide Gauge Observations

Tide Gauge	Trend (mm/yr)	
	Linear Regression	Harmonic Analysis
Antalya	+ 7.2 ± 0.6	+ 6.9 ± 0.4
Bodrum	+ 3.3 ± 0.6	+ 3.3 ± 0.6
Erdemli	+ 6.6 ± 4.7	+ 7.9 ± 2.9
İskenderun	+ 59.6 ± 6.0	+57.4 ± 3.3

Although the trends from linear regression and harmonic analysis are similar to each other, the trends from harmonic analysis are more appropriate for SLH nature. Since each tide gauge has different tidal constituents, significant constituents must be defined specially for each tide gauges. The difference of constituentsis taken into account by means of harmonic analysis process. Thus, to compare with altimetry vertical trends, the trends of harmonic analysis on MSL will be used in the process of extracting vertical trends and vertical crustal motions.

As mentioned before, vertical trends from altimetryobservations are defined from arithmetic mean of linear regression of chosen clusters. To remind, clusters have been chosen with respect to their similarity percentage. See Table 19 for vertical trends from altimetry observations.

Table 19 SSH Trends from Altimetry Observations

Pass Number	Chosen Clusters	Similarity Percentage	Trends (mm/yr)
68	03 – 07	86.61	+ 5.8 ± 1.5
159	04 – 08	84.60	+ 8.0 ± 1.5
170	03 – 07	90.28	+ 9.5 ± 1.3
246	04 – 08	86.60	+ 8.3 ± 1.5

After considering the trends from GPS, comparison of vertical trends will be made in this chapter at the last section. As the next step, GPS trends will be defined and investiaged in each station.

5.2 GPS Solution

The Global Positioning System (GPS) is a satellite positioning and navigation system that ensures time and locationinformation on or near the Earth. Note that there must be at least 4 GPS satellites in view to define position. It is maintained by the USA, and is available for anyone who has a GPS receiver. But there are some technical limitations which are only in use for military users.

To explain basically, the satellite is continually marked with own transmission time so that when received the signal transit period can be measured with a synchronized receiver. The original objectives of GPS were the instantaneous determination of position and velocity, and the precide coordination of time (Hofmann Wellenhof, Lichtenegger and Wasle 2008), (Chen and Lee 2001). Since there is a wide range of information about GPS technique at different resources, detailed information will not be given in this study.

Used GPS velocities have some drawbacks to use in comparison process of vertical crustal motion. First one, the GPS velocities are not derived from continuously operated observations. Latter one is that GPS campaigns are not regular and do not cover observation years of neither tide gauges, nor satellite altimetry. For some of tide gauges, GPS observations have been done from the point which is not on the tide gauge. It is realized as another disadvantage of GPS observations. Thus, GPS vertical trends will be evaluated seperately on the process of extracting vertical motion. The GPS campaigns which isused to derive coordinate velocities can be reached in Table 20.

Table 20 The Years of GPS Campaigns

TG/Years	1994	1995	1996	1997	1998	2001	2002	2003	2005	2006	2007	2008	2009
Antalya	X	X	X	X	X	X	X	X	X	X		X	X
Bodrum												X	X
Erdemli							X		X	X	X	X	X
İskenderun									X	X	X		X

Due to having only two years of GPS measurements on Bodrum tide gauge, the trends of Bodrum tide gauge are not taken into account at the stage of vertical trends comparison. Instead of the trends based on measurement of 2008 and 2009 years, the trends which are based on between 1994 and 2002 years from (Yıldız, et al. 2003) have been applied to see trends of MSL for Bodrum tide gauge. This value is +1.4mm/yr.

The GPS observations have been obtained with its position and velocities from data provider, GCM. Given GPS coordinates and their velocities can be seen in Table 21.

Table 21 GPS Positions and Trends

NOKTA	X(m)	Y(m)	Z(m)	Vx(mm/yr)	Vy(mm/yr)	Vz(mm/yr)
ANT	**4399214.608**	**2602657.597**	**3802195.036**	**-0.01072**	**0.00284**	**0.00408**
ERD	**4239347.195**	**2887013.214**	**3778606.012**	**-0.01109**	**0.00101**	**0.01967**
ISK	**4138373.371**	**3026637.283**	**3781263.849**	**-0.05039**	**-0.01769**	**-0.01741**

To define the vertical crustal motion on land, altitude must be computed from these coordinates and their velocities. Thus, these cartesian coordinates have been transformed to geodetic coordinates latitude (φ), longitude (λ), and altitude (h) (Rummel and Peters 2001).To run transformation, WGS84 parameters have been entered into ECEF2LLA.m program, then geodetic coordinates for each station have been computed respectively. Additionally, to see the vertical velocities of the considered

tide gauges, velocities given in cartesian coordinates have been translated into geodetic coordinates, WGS84.

The translation has been made by means of the formula below (Torge 2001)

$$\boldsymbol{x} = \boldsymbol{A^{-1}\Delta X} \tag{5.2}$$

Hereby,

$$\boldsymbol{A^{-1}} = \begin{bmatrix} -sin\varphi\cos\lambda & -\sin\varphi\sin\lambda & cos\varphi \\ -sin\lambda & cos\lambda & 0 \\ \cos\varphi\cos\lambda & \cos\varphi\sin\lambda & sin\varphi \end{bmatrix} \tag{5.3}$$

And,

$$\boldsymbol{\Delta X} = \begin{matrix} V_x \\ V_y \\ V_z \end{matrix} \tag{5.4}.$$

Resulted velocities can be seen in Table 22.

Table 22 GPS Velocities

Tide Gauge	Δφ (mm/yr)	Δλ (m/yr)	Δh (m/yr)
Antalya	+7.9	+7.9	-3.8
Erdemli	+20.9	+7.1	+4.8
İskenderun	+16.5	+15.5	-51.4

As it is seen from the Table 21 except for Antalya tide gauge, the tide gauges used in this study have huge amount of gaps. The comparison of vertical trends has been made at the next section of this chapter.

5.3 Determination of Sea Level Trends and Vertical Land Motions

Following the procedure explained through this study thus far, differential sea level trends between tide gauges and altimetry observations are calculated. Also, GPS trends have been considered seperately to see

vertical motions in each stations. Relevant results have been shown in Table 23.

Table 23 Comparison of Vertical Trends

Pass No.	Station	Satellite Altimetry (ALT)		Tide Gauges (TG)		ALT-TG (mm/yr)	GPS Solution Trend (mm/yr)	ALT-(TG+GPS) (mm/yr)
		Time Span	Trend(mm/yr)	Time Span	Trend(mm/yr)			
246	Antalya	1999.1-2009.1	+ 8.3 ± 1.5	1985.11-2010.12	+ 6.9 ± 0.4	+1.4	-3.8	+ 5.2
170	Bodrum	1999.1-2009.1	+ 9.5 ± 1.3	1985.12 – 2010.12	+ 3.3 ± 0.6	+6.2	+1.4	+4.8
68	Erdemli	1999.1-2009.1	+ 5.8 ± 1.5	2003.1-2010.12	+ 7.9 ± 2.9	-2.1	+4.8	-6.9
159	Iskenderun	1999.1-2009.1	+ 8.0 ± 1.5	2005.1-2010.12	+57.4 ± 3.3	-49.4	- 51.4	+2.0
Mean						-11.0	-12.3	+1.3

(a) SSH Trends obtained from the most similar group of clusters

Table 23 (Continued)

Pass No.	Station	Satellite Altimetry (ALT)		Tide Gauges (TG)		ALT-TG (mm/yr)	GPS Solution Trend (mm/yr)	ALT-(TG+GPS) (mm/yr)
		Time Span	Trend(mm/yr)	Time Span	Trend(mm/yr)			
246	Antalya	1999.1-2009.1	+6.2 ± 1.2	1985.11-2010.12	+ 6.9 ± 0.4	-0.7	-3.8	-3.1
170	Bodrum	1999.1-2009.1	+5.6 ± 1.2	1985.12 – 2010.12	+ 3.3 ± 0.6	+2.3	+1.4	-0.9
68	Erdemli	1999.1-2009.1	+5.2 ± 1.2	2003.1-2010.12	+ 7.9 ± 2.9	-2.7	+4.8	-7.5
159	Iskenderun	1999.1-2009.1	+6.6 ± 1.1	2005.1-2010.12	+57.4 ± 3.3	-50.8	- 51.4	+0.6
Mean						-13.0	-12.3	-2.7

(b) SSH Trends obtained from all clusters except for last three ones

CHAPTER 6

RESULTS

6.1 Discussion on Trend Progress

In this study, SSH trends, SLH trends and GPS vertical crustal trends have been compared with each other. The study shows that altimetry and tide gauge vertical trends are coherent to each other, and give vertical positive trends for Mediterranean coast of Turkey. This means that sea level is rising every year more or less 7 mm at the Mediterranean coast of Turkey.

It is required to mention that even though GPS trends have been used to understand vertical land motion in the study area, these values are not reliable due to only having velocities rather than observations. Also, the method which is used to extract SLH trends from tide gauges is accepted as appropriate one, however, time span of data collection is not quite enough to use harmonic analysis method due to not being revealed long term periods. It is suggested that there must be at least a decade of MSL values for a tide gauge, however, İskenderun and Erdemli Tide Gauges do not have at least a decade of time span.

As it is mentioned in related part of this study, data gaps of tide gauges have been fulfilled by means of hourly outputs of predicted signal values because of monthly existing MSL consistency between PSMSL data and calculated MSLs. However, it is suggested that for data gap first of all the difference between predicted values and calculated values must be taken. Then, for a gapped data time, the closest data must have been defined to

apply linear interpolation for gapped time. Lastly, linear interpolation value must be added to predicted value. Note that this method is valid for less than 24 hour data gaps.

For altimetry measurements, PCA similarity approach has been used to see SSH trends. This method is a kind of useful approach to see common behavior of SSH trendsgroup by group. Moreover, it gives an advantage to work on shallow water for SSH trends due to showing similarity of each clusters which are collected in a group.

On the other hand, using a group of five clusters decreases the measurements which have been obtained from altimetry missions. To illustrate, for Pass 68, there are available 10850 observations extracted from the missions, but only chosen 1750 observations have been used to define SSH trends in Table 23 (a). This situation is due to working in shallow water areas. Assuming that SSH must be homogenus in 30 km distance, after getting the most similar group resulted from PCA method,it can be said that consistent data is available to extract SSH trends, and in this way, coastal effect on SSH observations are investigated as well. On the other side, except for last three clusters, all clusters have been considered to figure out SSH trends for each pass. It is worthwhile to mention that the SSH trend differences between Table 23 (a) and (b) are mainly due to location difference of used clusters.

GPS velocities can be used to see the vertical motion of crust. However, these velocities must be obtained from continuous GPS (CGPS) observations. In this study, because of not having CGPS observations, there is no statistical investigation in GPS solutions. Therefore, GPS vertical velocities derivede from Episodic GPS (EGPS) observations have been evaluated seperately in the process of extracting vertical trends.

6.2 Evaluation of the Results

As it is seen from the Table 23 (a) and (b), SSH trends are deviating from each other mostly 3.8 mm, and 1.4 mm respectively. There are some reasons acting on SSH trends cause these milimetric trend differences. These can be summarized as follow

- Meteorological effects like wind, pressure,
- Measurement accuracy,
- Slope of sea,
- Bathymetry,
- Unmodeled instrumental errors,
- Lack of global correction,
- Local salinity and temperature differences.

Besides, SLH trends derived from tide gauges deviates much more than SSH trends. The main reason is that as the main subject of this study tide gauges measure sea level, due to being set up on the Earth crust, they detect both sea surface height variations and vertical crustal movements. Also, meteorologic observations are required to see the effect of them on SLH variations.

Although T test results ontrend parameters show that the trends deduced from Erdemli and İskenderun tide gauges are statistically significant, it is suggested that tide gauge observations must cover at least a decade to figure out vertical SLHs confidently. Because of some tidal effects acting on SLH trends significantly can be extracted by 10 years hourly SLH data. Thus, these effects must be defined and removed from MSL trends.

For Table 23 (a), looking at Antalya and related Pass, Pass 246,denotes difference +1.4 mm which means that tide gauge location goes up, however, GPS solution does not agree with this trend. It can be due to not having CGPS measurements. Also, if the clusters from 19 to 23 would be considered to calculate SSH trends which are more closer than used

clusters sea level trend would be +3.6 mm/yr. This means that consistent result would be available with sea level trends deduced from Antalya tide gauge. However, due to not having the most similar behavior from these clusters, this result is not put into vertical trend comparison table. Note that the distance between five clusters which are used to have SSH trends and Antalya tide gaugeis far by 202 km, can be a part of reason for that difference. On the other side, Table 23 (b) represents consistent result with GPS solution. If the vertical trend deduced from GPS velocity is correct, it can be said that shallow water acts on SSH observations only 25 km near with coastal side of Antalya station.

It is seen that tide gauge location moves up +6,2 mm every year with respect to ALT-TG difference between Pass 170 and Bodrum tide gauge vertical trends in Table 23 (a). Also, GPS solution shows that there is a trend equals to +1.4 mm for each year. The results represent consistency, but there is no considerable vertical movement of Bodrum station. Considering Table 23 (b) gives more consistent result than the most similar group approach. In these aspects, it can be confidently said that the Bodrum station goes up gradually.

As third station, Erdemli is evaluated with Pass 68 of satellite altimetry missions. For Table 23 (a), SSH has +5.8 mm trend in a year, on the other hand, Erdemli station gives +7.9 mm value. It is shown that Erdemli tide gauge decreases in amount of - 2.1 mm each year. But, EGPS solution shows +4.8 mm trend for Erdemli station. This difference, like Antalya tide gauge, can be both resulted from distance between Erdemli station and chosen clusters, and lack of continuous GPS observations. Also, note that tide gauge observation time span and data gaps can not give enough outputs to detect vertical crustal motion confidently. Last but not least thing, some GPS observations instead being observed on tide gauge point, gathered on a close location to the tide gauge. Both local crustal movement differences between GPS and

tide gauge points and absence of meteorological observations can cause this dilemma for the trend solution. Note thin Table 23 (b) SSH trends deduced from altimetry observations give more or less the same result with Table 23 (a) for Pass 68.

As the last tide gauge, İskenderun station is handled with Pass 159. Although having only for 6 years observations on İskenderun station, it is seen that this tide gauge rises sharply. Altimetry observations show the +8.0 and +5.2 mm trend Table 23 (a) and (b) for each year, however, İskenderun tide gauge represents +57.4 mm trend. GPS processing result points that İskenderun tide gauge decreases 51.4 mm in a year. This means that there is a huge amount of vertical crustal motion for İskenderun tide gauge. Also, there is a high level consistency on vertical trends between altimetry, tide gauge and EGPS velocities. This station must be observed with continuous GPS receiver to detect its velocity regularly. If it is possible, the tide gauge station can be relocated to the place where is tectonically less active.

CHAPTER 7

CONCLUSION AND RECOMMENDATIONS

In this study, SSH derived from altimetry missions have been used to see sea level variations in space and time. Due to time resolution and time span of advantage, Jason-1 and T/P missions have been chosen as reference altimetry satellites. Clustering process was the first step of this study on altimetry data, as second step quality control has been made by means of Pope and T test approaches. Then, each observation is relocated to related center with respect to geoid height difference between cluster center and measurement positions. To apply PCA method, each cluster has been analyzed and interpolated as time series within frequency and time domain methods. Thus, PCA method has been implemented in time series in each cluster to figure out similarities of them. Moreover, all clusters except for last three ones have been used to consider the change of SSH trend values in each Pass as well.

Also, tide gauge data obtained from GCM has been analyzed to reveal tidal constituents and fulfill data gaps in hourly data. Four stations have been evaluated which are lengthening at the Mediterranean coast of Turkey. Then, to extract daily and monthly MSL values of each tide gauge a 119 point convolution filter has been used to do so. Monthly MSL data obtained from PSMSL have been fulfilled with calculated MSL values. Afterwards, SLH trends have been computed by means of both linear regression and harmonic analysis.

To have more convenient vertical trends EGPS solution has been considered. So that vertical trends and probable error resources were

under inspection to figure out advantages and disadvantages of considered data and methods.

To select the proper outlier detection method PEB value has been applied to SSH data. It is seen that Pope outlier test gives dominantly better results than Interquartile method with respect to PEB value. Also, relaocating SSHs by geoid height to their centers reduced the standard deviation of each cluster significantly. To sum up, Pope test as an outlier detection method and geoid height as reference height to relocate SSH values are useful tools to implement in SSH values. So that all measurements are brought to their centers correspondingly.

The future work deduced from this study has been mentioned at the following part.

Although Jason-1 and T/P has better time resolution than ENVISAT mission, there is a mission called ENVISAT which has better spatial resolution than the Jason-1 and T/P. Because of calling for continues observations covering at least ten years in study area, ENVISAT has not been chosen as reference altimetry mission in this study. However, two years later there can be a study to work with ENVISAT for seeing SSH trends and comparing them with tide gauge observations in the study area.

To cluster SSH observations, K-means clustering method has been applied to the data. As mentioned before, cluster numbers have been entered manually into operation. Thus, clustering process which is based on K-means method must be automated by developing an algorithm to define cluster numbers automatically. Also, if cluster numbers become more than 28, all data must be divided into two parts for K-means clustering process. There can be study to perform these tasks automatically.

After application of frequency domain analysis of SSH data set, the dominant periods have been defined in data. These periods are for 1, 2,

6, 8 years, clearly, exact values are available in appendices. So that it can be said that some local tidal effects which are not extracted by global ocean tide model (GOT 4.7) can be still existing in corrected SSH observations for Mediterranean Sea.

Since the study area is known as shallow water, PCA method has been implemented in data to see common behavior of clusters in time. Also, bathymetric data can give information to figure out the relation between cluster similarities and bathymetry. So that proper clusters can be chosen by means of bathymetry data in this area. Also, to make decision about sufficient amount of similarity percentage to extract SSH trends can be defined with further studies. Then, there may be no need to take the best similar group which is sometimes so far from tide gauge station. In this aspect, there can be some studies to improve GOT 4.7 for Mediterranean Sea.

Although four tide gauges have been investigated in this study, some of which had both an amount of MSL data gap and short time span. It would be quite well if there would have been continuos observations covering at least a decade,however, used hourly data do not meet with this condition.Moreover, Doodson number sets are used to define tidal constituents from hourly data, instead of this number set, some different number sets can be applied to the hourly data to get more constituents and see its effects on SLH trends in each station.As mentioned before, meteorological measurements must have been taken to model the effects like wind, pressure etc.

As last but not least thing, there is a service which is called CORS-TR to perform observations on GNSS satellites. To have continues observations this system can be used to collect position data of each tide gauge. Also, GPS observations must be done exactly on the same location of tide gauges to separate crustal motions from SLH trends precisely.

REFERENCES

(SLC), University of Hawaii. *Hawaii Uni.* http://ilikai.soest.hawaii.edu/UHSLC/jaslsoft2.html (accessed 11 07, 2011).

Allison, Paul D. *Logistic Regression Using the SAS System.* SAS Institute, 1999.

AVISO. *Product.* April 2011. ftp://ftp.aviso.oceanobs.com/pub/oceano/AVISO/SSH/monomission/dt (accessed August 30, 2011).

AVISO, Handbook. *DT CorSSH and DT SLA Product Handbook.* AVISO, 2011.

Ball, G., and D. Hall. "A Clustering Technique for Summarizing Multivariate Data." *Behavioral Science*, 1967: 153-155.

Barnett, T.P. "The Estimation of "global" sea level change: a problem of uniqueness." *Journal of Geophysical Research*, 1984: 7980-7988.

Barnett, V., and T. Lewis. *Outliers in Statistical Data.* John Wiley & Sons., 3rd edition, 1994.

Benveniste, Jérôme, and Nicolas Picot. *Radar Altimetry Tutorial.* ESA, CNES, 2011.

Birney, D.S., G. Gonzalez, and D. Oesper. *Observational Astronomy.* Cambridge University Press, 2006.

Bosch, Wolfgang, and Roman Savcenko. *BIN data structure - altimeter data reorganized for time series analysis.* Münich: Deutsches Geodatisches Forschungsinstitut, 2005.

Braitenberg, Carla, Patrizia Mariani, Lavinia Tunini, Barbara Grillo, and Ildiko Nagy. "Vertical Crustal Motions from Differential Tide Gauge Observations and Satellite Altimetry in Southern Italy." *Journal of Geodynamics*, 2010.

CalVal, AVISO. *AVISO CalVal.* 2011. http://www.aviso.oceanobs.com/en/newsstand/newsletter/newsletter07/jason-1-calibrationvalidation/index.html (accessed 11 05, 2011).

Carrera, G., and P. Vanicek. "The Use of Sea Level Tide Gauge Observations in Geodesy." *Lighthouse Edition*, 1985: 13-16.

Chen, Y.Q., and Y.C. Lee. *Geographical Data Acquisition.* Wien: Springer-Verlag, 2001.

Colorado University SLR, Sea Level Research Group. 2011. http://sealevel.colorado.edu/content/tide-gauge-sea-level (accessed September 1, 2011).

De Boor, C. *A Practical Guide to Splines.* Springer, 2001.

Douglas, Bruce C. "Global Sea Level Change: Determination and interpretation." *Reviews of Geophysics*, 1995: 1425-1432.

eHow. *eHow.* 2011. http://www.ehow.com/how_4546238_calculating-percentage-error.html (accessed September 1, 2011).

ESA, and CNES. *Basic Radar Altimetry Toolbox v3.0 User Manual.* ESA, CNES, 2011.

ESEAS. *Description of Scientific/Technological Objectives and Work Plan, Part B, First Draft of Proposal for Support for Research Infrastructure.* European Sea Level Service, 2001.

Fu, Lee-Lueng, and Anny Cazenave. *Satellite Altimetry and Earth Sciences.* California: ACADEMIC PRESS, 2001.

Garcia, D, I. Vigo, B.F. Chao, and M.C. Martinez. "Vertical Crustal Motion Along the Mediterranean and Black Sea Coast Derived from Ocean Altimetry and Tide Gauge Data." *Pure and Applied Geophysics*, 2007: 851-863.

Govaert, Gerard. *Data Analysis.* Wiley, 2009.

Groger, M., and H. Plag. "Estimations of a Global Sea Level Trend: Limitations from the Structure of the PSMSL Global Sea Level Data Set." *Global and Planetary Change*, 1993: 161-179.

H., William, Saul A. Teukolsky, William T. Vetterling, and Brian P. Flannery. *Numerical Recipes in C Example Book : The Art of Scientific Computing.* New York: Cambridge Press, 1992.

Hofmann Wellenhof, B., H. Lichtenegger, and E. Wasle. *Global Navigation Satellite Systems.* Springer Wien NewYork, 2008.

Hubbard, R. *Boater's Bowditch: The Small Craft American Practical Navigator.* International Marine, 1997.

Ibanoglu, C. *Variable Stars as Essential Astrophysical Tools.* Springer, 2000.

IOC, Intergovernmental Oceanographic Commission. *Manual on Sea Level Measurement amd Interpretation: Reappraisals and Recommendetions as of the Year 2000, Manual and Guides.* Paris, 2000.

JCOMM, Intergovernmental Oceanographic Commision. *Manual on Sea Level Measurement and Interpretation.* JCOMM, 2006.

Koch, Karl Rudolf. *Parameter Estimation and Hypothesis Testing in Linear Models.* Springer, 1999.

Kuo, C.Y., C.K. Shum, Alexander Braun, Kai-Chien Cheng, and Yuchan Yi. "Vertical Motion Determined Using Satellite Altimetry and Tide Gauges." *Terrestrial, Atmospheric and Oceanic Sciences*, 2008.

Kuo, Chung-Yen, and C.K Shum. "Vertical Crustal Motion Determined by Satellite Altimetry and Tide Gauge Data in Fennoscandia." *Geophysical Research Letters*, 2004.

LEX, Transnational College of. *Who is Fourier ? A Mathematical Adventure.* Language Research Foundation, 2006.

Lilley, D.G. *Numerical Methods.* Stillwater, 2002.

LombScargle. *LombScargle Mathworks.* http://www.mathworks.com/matlabcentral/fileexchange/993 (accessed 11 08, 2011).

MacQueen, J.B. "Some Methods for Classification and Analysis of Multivariate Observations." *Proc. Symp. Math. Statist. and Probability (5th)*, 1967: 281-297.

Mangiarotti, S. "Coastal Sea Level Trends from TOPEX-Poseidon Satellite Altimetry and Tide Gauge Data in the Mediterranean Sea During the 1990s." *Geophysical Journal International*, 2007: 132-144.

Marc, L. Fenoglio. "Long-term Sea Level Change in the Mediterranean Sea from Multi-Satellite Altimetry and Tide Gauges." *Physics and Chemistry of the Earth*, 2002: 1419-1431.

Marc, L.F., C. Dietz, and E Groten. "Vertical Land Motion in the Mediterranean Sea from Altimetry and Tide Gauge Stations." *Marine Geodesy*, 2004: 683-701.

Mitchum, G. T. "Comparison of T/P Sea Surface Heights and Tide Gauge Sea Levels." *Journal of Geophysical Research*, 1994.

Nerem, R. S., and G. T. Mitchum. "Estimates of Vertical Crustal Motion Derived from Differences of TOPEX/POSEIDON and Tide Gauge Sea Level Measurements." *Geophysical Research Letters*, 2002.

Nerem, R.S., R. J. Eanes, J.C. Ries, and G.T. Mitchum. "The Use of a Precise Reference Frame for Sea Level Change Studies." *International Association of Geodesy*, 1998.

O'Neill, C. *Cubic Spline Interpolation.* 2002.

Pavlis, N.K., S.A. Holmes, S.C. Kenyon, and J.K. Factor. "An Earth Gravitational Model to Degree." *2008 General Assembly of the European Geosciences Union.* EGU, 2008.

Pawlowicz, R., B. Beardsley, and S. Lentz. *Classical Tidal Harmonic Analysis Including Error Estimates in MATLAB using T_TIDE.* 2002.

Press, W.R., B.P. Flannery, S.A. Teukolsky, and W.T. Vetterling. *Numerical Recipes.* Cambridge University Press, 2007.

PSMSL. 2011. http://www.psmsl.org/ (accessed August 29, 2011).

Pugh, D.T. *Tides, Surges and Mean Sea Level.* John Wiley and Sons Ltd. Wiley, 1987.

Rauscher, Christoph, Volker Janssen, and Roland Minihold. *Fundamentals of Spectrum Analysis.* Münich: Rohde & Schwarz, 2001.

Reddy, M.P.M., and M. Affholder. *Descriptive Physical Oceanography.* Taylor and Francis, 2002.

Rummel, R., and T. Peters. *Reference Systems in Satellite Geodesy.* München: Institut für Astronomische und Physikalische Geodäsie, 2001.

Savransky, Dmitry. *LOMB.* May 21, 2008.

Shlens, J. *A Tutorial on Principal Component Analysis.* New York University, 2009.

Smith, Lindsay. *Tutorial on Principal Component Analysis.* February 26, 2002.

Tiwari, Kunal, Krishna Mehta, Nitin Jain, and Ramandeep,Kanda,Gaurav Tiwari. "Selecting the Appropriate Outlier Treatment for Common Industry Applications." *Statistics and Data Analysis*, 2007.

TOGA, Hawaii University. *Hawaii University.* http://ilikai.soest.hawaii.edu/UHSLC/jaslpr2/slman2.html (accessed 12 02, 2011).

Torge, W. *Geodesy.* New York: Walter de Gruyter, 2001.

Upton, Graham, and Ian Cook. *Understanding Statistics.* Oxford University Press., 1996.

Wolberg, J. *Data Analysis Using the Method of Least Squares.* Sprigner, 2006.

Xu, Rui, and Donald C. Wunsch II. *Clustering.* New Jersey: John Wiley & Sons, 2009.

Yıldız, H., C. Demir, M.A. Gürdal, O.A. Akabalı, M.E. Ayhan, and Y. Türkoğlu. "Harita Dergisi." *Analysis of Sea Level And Geodetic Measurements Of Antalya-II, Bodrum II, Erdek and Menteş Tide Gauges in The Period Of 1984-2002*, June 2003.

Yıldız, Hasan. *Determination of Mean Sea Level and Vertical Crustal Movements by Using Sea Level and Geodetic Measurements.* Ankara: METU, 2001.

Yıldız, Hasan. *Mareograf ve Sabit GPS Verileri ile Uzun Dönemli Mutlak Deniz Seviyesi Değişimlerinin Araştırılması.* Doktora Tezi: İstanbul Teknik Üniversitesi, 2005.

APPENDIX A

Flow Chart of The Study

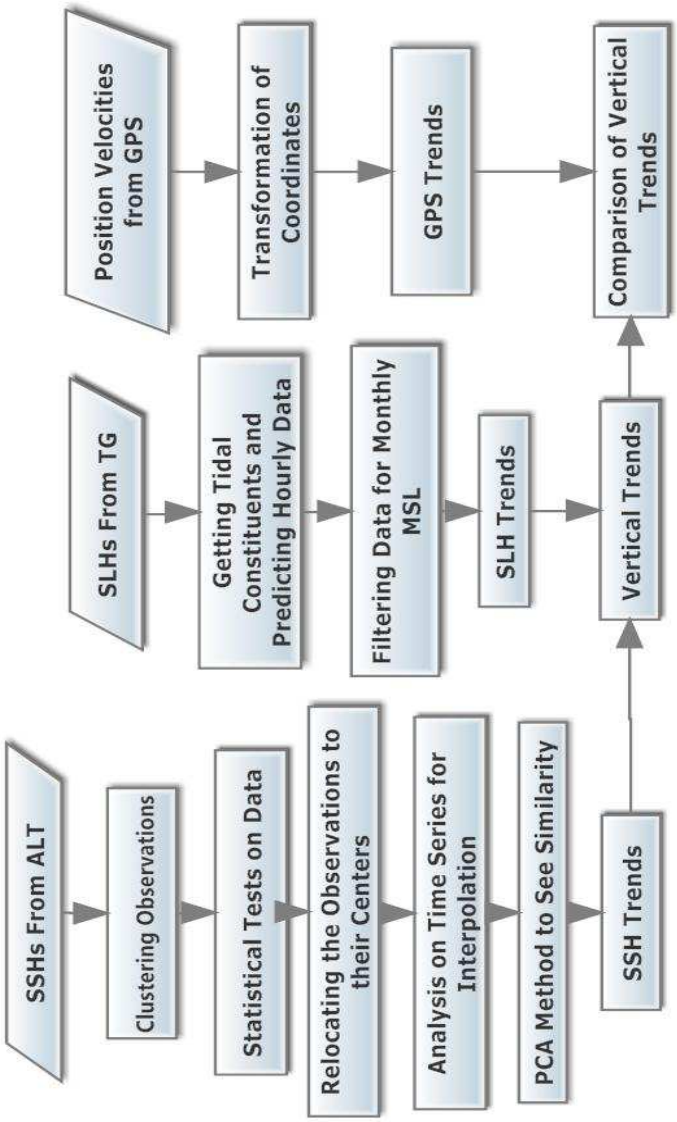

Figure 16 Flowchart of the Study

APPENDIX B

Clusters of Altimetry Observations

(Pass:68, 159, 170. 246 respectively)

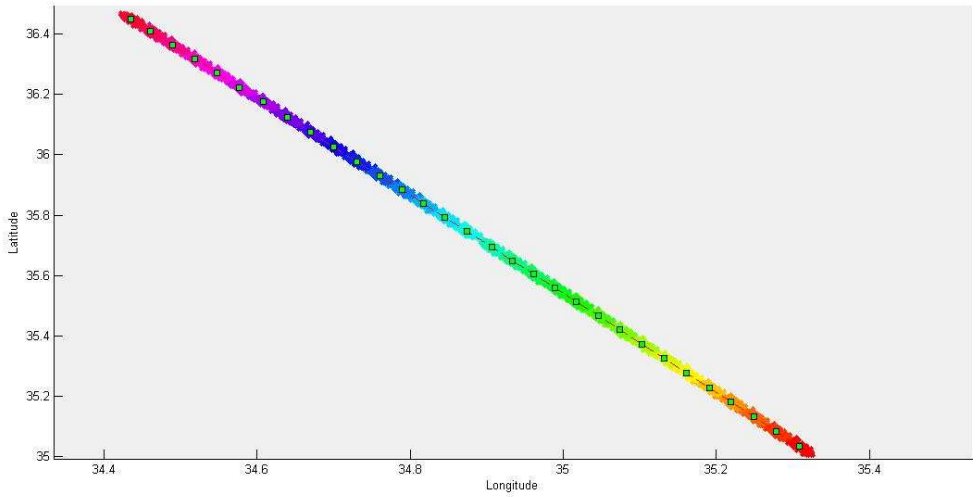

Figure 17 Clusters of Pass 68

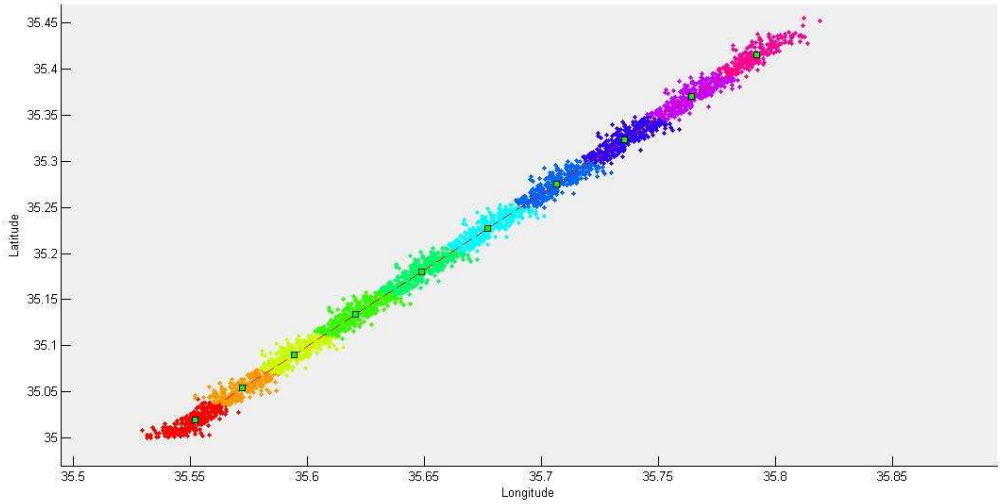

Figure 18 Clusters of Pass 159

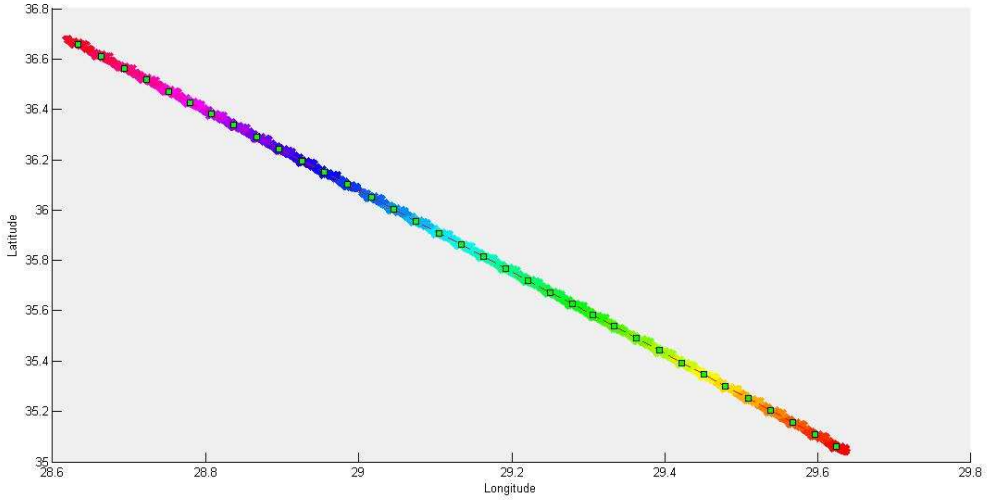

Figure 19 Clusters of Pass 170

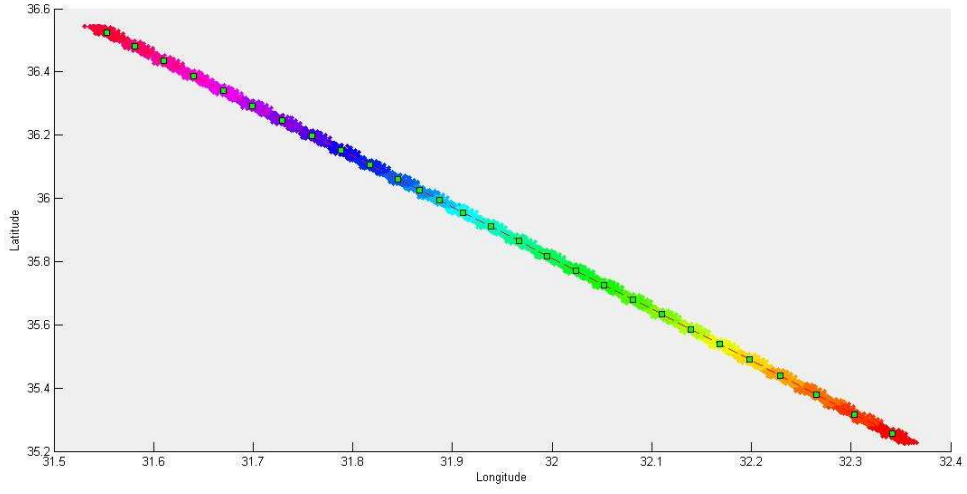

Figure 20 Clusters of Pass 246

APPENDIX C

Cluster Similarities

Table 24 Pass 68 Cluster Similarities

Pass No.	Clusters	Percentage
68	27 - 31	65.88
	26 – 30	71.29
	25 - 29	76.95
	24 - 28	79.88
	23 - 27	80.62
	22 - 26	81.24
	21 - 25	81.92
	20 – 24	81.90
	19 – 23	81.26
	18 – 22	79.81
	17 – 21	79.94
	16 – 20	80.65
	15 - 19	79.94
	14 – 18	80.78
	13 – 17	80.92
	12 – 16	79.86
	11 – 15	78.67
	10 – 14	79.50
	09 – 13	80.10
	08 – 12	83.69
	07 – 11	84.14
	06 – 10	86.24
	05 – 09	86.44
	04 – 08	85.85
	03 – 07	86.61
	02 – 06	86.42
	01 - 05	85.49

Table 25 Pass 159 Cluster Similarities

Pass No.	Clusters	Percentage
159	06 - 10	76.28
	05 - 09	83.44
	04 – 08	84.60
	03 – 07	81.07
	02 – 06	73.54
	01 - 05	65.51

Table 26 Pass 170 Cluster Similarities

Pass No.	Clusters	Percentage
170	31 – 35	65.27
	30 – 34	71.14
	29 – 33	73.44
	28 – 32	74.78
	27 – 31	74.97
	26 – 30	76.81
	25 – 29	79.66
	24 – 28	78.93
	23 – 27	80.37
	22 – 26	81.96
	21 – 25	82.48
	20 – 24	83.04
	19 – 23	85.26
	18 – 22	85.47
	17 – 21	87.35
	16 – 20	86.44
	15 – 19	87.22
	14 – 18	85.67
	13 – 17	84.26
	12 – 16	81.37
	11 – 15	80.56
	10 – 14	80.62
	09 – 13	81.00
	08 – 12	83.34
	07 – 11	86.99
	06 – 10	89.10
	05 – 09	89.46
	04 – 08	89.66
	03 – 07	90.28
	02 - 06	89.81
	01 – 05	88.85

Table 27 Pass 246 Cluster Similarities

Pass No.	Clusters	Percentage
246	24 – 28	69.66
	23 – 27	72.68
	22 – 26	74.96
	21 – 25	77.80
	20 – 24	76.26
	19 – 23	76.61
	18 – 22	73.99
	17 – 21	65.86
	16 – 20	59.37
	15 – 19	57.99
	14 – 18	56.75
	13 – 17	61.17
	12 – 16	71.78
	11 – 15	76.73
	10 – 14	82.02
	09 – 13	84.31
	08 – 12	85.08
	07 – 11	84.26
	06 – 10	84.96
	05 – 09	85.39
	04 – 08	86.60
	03 – 07	86.01
	02 - 06	85.61
	01 - 05	84.37

APPENDIX D

Cluster Trends

(Pass 68, 159, 170. 246 respectively. Unit is mm. for trends and std.)

Table 28 Cluster Trends of Pass 68

t table value	1.28
1 trend 6.1 ± 1.5 t_test	4.06
2 trend 5.7 ± 1.5 t_test	3.78
3 trend 6.6 ± 1.5 t_test	4.40
4 trend 4.5 ± 1.5 t_test	3.09
5 trend 5.2 ± 1.5 t_test	3.53
6 trend 6.2 ± 1.5 t_test	4.15
7 trend 6.3 ± 1.5 t_test	4.22
8 trend 5.9 ± 1.5 t_test	4.03
9 trend 6.3 ± 1.5 t_test	4.15
10 trend 7.7 ± 1.5 t_test	5.08
11 trend 5.5 ± 1.5 t_test	3.52
12 trend 5.9 ± 1.5 t_test	3.98
13 trend 5.1 ± 1.4 t_test	3.61
14 trend 6.5 ± 1.4 t_test	4.55
15 trend 5.3 ± 1.4 t_test	3.71
16 trend 6.3 ± 1.5 t_test	4.26
17 trend 5.9 ± 1.5 t_test	4.00
18 trend 4.1 ± 1.5 t_test	2.72
19 trend 5.3 ± 1.6 t_test	3.35
20 trend 6.3 ± 1.5 t_test	4.25
21 trend 4.2 ± 1.5 t_test	2.71
22 trend 5.6 ± 1.5 t_test	3.71
23 trend 3.4 ± 1.5 t_test	2.35
24 trend 3.9 ± 1.4 t_test	2.70
25 trend 3.7 ± 1.5 t_test	2.48
26 trend 2.9 ± 1.4 t_test	2.02
27 trend 3.1 ± 1.6 t_test	1.97
28 trend 2.6 ± 1.6 t_test	1.59
29 trend 0.1 ± 1.5 t_test	0.09
30 trend-1.0 ± 1.6 t_test	0.62
31 trend-2.0 ± 1.3 t_test	1.51

Table 29 Cluster Trends of Pass 159

t table value1.28	
1 trend 2.3 ± 1.3 t_test	1.77
2 trend 4.4 ± 1.3 t_test	3.45
3 trend 5.3 ± 1.4 t_test	3.80
4 trend 6.8 ± 1.4 t_test	4.84
5 trend 7.2 ± 1.4 t_test	5.22
6 trend 9.2 ± 1.4 t_test	6.32
7 trend 8.8 ± 1.5 t_test	5.94
8 trend 8.1 ± 1.5 t_test	5.30
9 trend 6.0 ± 1.5 t_test	4.05
10 trend 2.4 ± 1.5 t_test	1.66

Table 30 Cluster Trends of Pass 170

t table value	1.28
1 trend 8.5 ± 1.3 t_test	6.76
2 trend 8.8 ± 1.3 t_test	6.94
3 trend 9.1 ± 1.2 t_test	7.25
4 trend 8.9 ± 1.3 t_test	7.08
5 trend 9.5 ± 1.3 t_test	7.30
6 trend 10.4 ± 1.3 t_test	7.88
7 trend 9.4 ± 1.3 t_test	7.05
8 trend 8.9 ± 1.3 t_test	6.60
9 trend 8.3 ± 1.3 t_test	6.14
10 trend 9.3 ± 1.3 t_test	6.94
11 trend 7.5 ± 1.3 t_test	5.58
12 trend 5.2 ± 1.3 t_test	4.10
13 trend 6.3 ± 1.4 t_test	4.65
14 trend 6.4 ± 1.4 t_test	4.57
15 trend 7.6 ± 1.4 t_test	5.44
16 trend 5.0 ± 1.4 t_test	3.53
17 trend 5.1 ± 1.4 t_test	3.66
18 trend 5.5 ± 1.4 t_test	3.90
19 trend 4.5 ± 1.4 t_test	3.17
20 trend 3.7 ± 1.4 t_test	2.61
21 trend 3.4 ± 1.4 t_test	2.42
22 trend 2.9 ± 1.4 t_test	2.09
23 trend 2.4 ± 1.4 t_test	1.70
24 trend 3.0 ± 1.5 t_test	2.08
25 trend 2.3 ± 1.5 t_test	1.54
26 trend 3.6 ± 1.5 t_test	2.40
27 trend 2.9 ± 1.5 t_test	1.92
28 trend 2.2 ± 1.6 t_test	1.40
29 trend 2.2 ± 1.5 t_test	1.51
30 trend-0.1 ± 1.5 t_test	0.10
31 trend 1.6 ± 1.5 t_test	1.04
32 trend 1.7 ± 1.6 t_test	1.12
33 trend 0.6 ± 1.6 t_test	0.40
34 trend-0.9 ± 1.6 t_test	0.55
35 trend-2.7 ± 1.6 t_test	1.70

Table 31 Cluster Trends of Pass 246

t table value	1.28
1 trend 6.9 ± 1.4 t_test	4.83
2 trend 7.8 ± 1.4 t_test	5.43
3 trend 8.3 ± 1.5 t_test	5.61
4 trend 9.1 ± 1.5 t_test	6.17
5 trend 8.1 ± 1.5 t_test	5.54
6 trend 7.0 ± 1.5 t_test	4.78
7 trend 7.8 ± 1.5 t_test	5.35
8 trend 9.6 ± 1.5 t_test	6.55
9 trend 9.1 ± 1.5 t_test	5.95
10 trend 8.1 ± 1.5 t_test	5.90
11 trend 8.1 ± 1.5 t_test	5.46
12 trend 7.8 ± 1.5 t_test	5.59
13 trend 6.6 ± 1.6 t_test	4.07
14 trend 6.1 ± 1.5 t_test	4.00
15 trend 6.5 ± 1.6 t_test	4.06
16 trend 5.1 ± 1.4 t_test	3.53
17 trend 2.6 ± 1.5 t_test	1.69
18 trend 4.6 ± 1.5 t_test	2.97
19 trend 4.9 ± 1.6 t_test	3.02
20 trend 3.2 ± 1.6 t_test	1.95
21 trend 3.1 ± 1.6 t_test	1.96
22 trend 4.1 ± 1.7 t_test	2.45
23 trend 2.9 ± 1.6 t_test	1.80
24 trend 1.6 ± 1.7 t_test	0.96
25 trend 2.7 ± 1.7 t_test	1.68
26 trend 0.4 ± 1.7 t_test	0.24
27 trend 3.7 ± 1.7 t_test	2.14
28 trend 0.3 ± 1.7 t_test	0.20

APPENDIX E

Standard Deviations of Clusters Before and After Centered

Std. Unit is cm

Table 32 Before and After Centered Standard Dev. of Pass 68

10.27	8.59
11.08	8.59
11.20	8.60
12.02	8.24
13.07	8.39
12.92	8.58
12.22	8.61
11.37	8.43
11.39	8.66
10.91	8.62
10.70	8.79
10.54	8.59
10.30	8.14
10.15	8.29
9.57	8.41
9.94	8.47
9.59	8.38
8.60	8.59
9.26	8.94
8.53	8.48
8.63	8.66
8.56	8.57
8.41	8.16
8.94	8.29
9.28	8.47
8.99	8.04
9.95	8.87
10.98	9.48
11.29	8.79
12.81	9.60
13.20	8.54

Table 33 Before and After Centered Standard Dev. of Pass 159

11.16	7.88
11.07	8.12
10.85	8.33
11.42	8.17
11.71	8.10
12.42	8.62
12.19	8.65
12.50	8.91
11.92	8.52
12.51	9.17

Table 34 Before and After Centered Standard Dev. of Pass 170

11.76	7.47
12.49	7.55
13.44	7.47
13.32	7.46
13.05	7.71
12.58	7.93
12.14	7.93
11.74	7.95
10.76	7.92
10.04	7.97
9.49	7.98
9.14	7.40
9.70	7.86
10.52	8.02
10.77	8.11
11.33	8.07
12.20	7.95
12.62	8.05
13.34	8.01
14.86	7.97
17.08	8.04
18.64	7.97
19.47	7.98
19.96	8.23
19.81	8.54
19.06	8.58
19.19	8.73
18.96	9.24
21.07	8.52
23.78	8.65
26.42	8.68
28.24	8.95
28.32	9.26
29.39	9.23
30.84	10.46

Table 35 Before and After Centered Standard Dev. of Pass 246

20.44	8.23
24.08	8.60
22.07	8.39
17.43	8.40
14.93	8.41
13.50	8.47
13.01	8.57
12.19	8.59
11.23	8.73
10.44	8.78
10.24	8.77
10.17	8.78
11.02	9.35
10.85	8.88
11.68	9.45
11.34	9.20
11.87	9.73
11.58	9.28
12.96	9.40
13.41	9.42
13.57	9.09
14.20	9.49
14.84	8.99
15.41	9.55
16.55	9.80
17.39	9.73
18.14	10.26
18.06	10.03

APPENDIX F

Geodetic Coordinates (WGS84) of Cluster Centers

Table 36 Geodetic Coor. of Cluster Cent. for Pass 68

Cluster Number	Latitude	Longitude
1	35.0341	35.3087
2	35.0842	35.2787
3	35.1333	35.2490
4	35.1817	35.2196
5	35.2294	35.1908
6	35.2777	35.1615
7	35.3257	35.1323
8	35.3731	35.1035
9	35.4203	35.0746
10	35.4676	35.0457
11	35.5148	35.0167
12	35.5604	34.9888
13	35.6053	34.9615
14	35.6499	34.9339
15	35.6946	34.9067
16	35.7466	34.8744
17	35.7933	34.8454
18	35.8388	34.8173
19	35.8836	34.7896
20	35.9307	34.7603
21	35.9781	34.7308
22	36.0270	34.7004
23	36.0766	34.6695
24	36.1253	34.6392
25	36.1754	34.6078
26	36.2239	34.5773
27	36.2709	34.5479
28	36.3179	34.5186
29	36.3644	34.4893
30	36.4090	34.4613
31	36.4493	34.4357

Table 37 Geodetic Coor. of Cluster Cent. for Pass 159

Cluster Number	Latitude	Longitude
1	35.0200	35.5517
2	35.0540	35.5721
3	35.0904	35.5942
4	35.1336	35.6202
5	35.1800	35.6484
6	35.2272	35.6770
7	35.2754	35.7062
8	35.3232	35.7354
9	35.3704	35.7639
10	35.4157	35.7917

Table 38 Geodetic Coor. of Cluster Cent. for Pass 170

Cluster Number	Latitude	Longitude
1	35.0595	29.6244
2	35.1070	29.5960
3	35.1548	29.5670
4	35.2030	29.5378
5	35.2514	29.5085
6	35.2992	29.4793
7	35.3467	29.4505
8	35.3938	29.4217
9	35.4418	29.3924
10	35.4900	29.3628
11	35.5377	29.3336
12	35.5822	29.3064
13	35.6274	29.2788
14	35.6731	29.2505
15	35.7204	29.2214
16	35.7676	29.1922
17	35.8145	29.1631
18	35.8616	29.1340
19	35.9088	29.1047
20	35.9562	29.0753
21	36.0040	29.0456
22	36.0510	29.0164
23	36.1014	28.9848
24	36.1485	28.9554
25	36.1960	28.9257
26	36.2431	28.8961
27	36.2906	28.8662
28	36.3377	28.8367
29	36.3836	28.8077
30	36.4280	28.7797
31	36.4719	28.7518
32	36.5173	28.7231
33	36.5643	28.6934
34	36.6113	28.6636
35	36.6588	28.6336

Table 39 Geodetic Coor. of Cluster Cent. for Pass 246

Cluster Number	Latitude	Longitude
1	35.2547	32.3411
2	35.3165	32.3036
3	35.3792	32.2650
4	35.4377	32.2294
5	35.4895	32.1978
6	35.5382	32.1680
7	35.5855	32.1390
8	35.6325	32.1101
9	35.6793	32.0812
10	35.7262	32.0523
11	35.7723	32.0238
12	35.8183	31.9953
13	35.8650	31.9665
14	35.9107	31.9382
15	35.9549	31.9105
16	35.9940	31.8865
17	36.0247	31.8672
18	36.0607	31.8449
19	36.1053	31.8169
20	36.1516	31.7881
21	36.1981	31.7589
22	36.2454	31.7293
23	36.2929	31.6993
24	36.3402	31.6697
25	36.3876	31.6398
26	36.4347	31.6102
27	36.4804	31.5815
28	36.5248	31.5530

APPENDIX G

Significant Periods of Each Cluster

Table 40 Significant Periods of Pass 68

1	1.00438356164384
2	1.00438356164384
3	1.00438356164384
4	1.29597878921785, 1.00438356164384
5	1.00438356164384
6	1.00438356164384
7	1.00150567123288
8	1.00438356164384
9	1.00438356164384
10	1.00150567123288
11	1.00438356164384
12	1.03013698630137
13	6.69589041095890. 1.00438356164384
14	1.03013698630137
15	1.03013698630137
16	1.00438356164384
17	1.00438356164384
18	5, 72288954990215, 1.00150567123288
19	6.69589041095890.1.00438356164384
20	5, 73933463796478, 1.00438356164384
21	5, 73933463796478, 1.00438356164384
22	1.03013698630137
23	6.67670447488584, 1.00150567123288
24	1.02718530382859
25	1.02423362135581
26	6.61914666666667, 0.992872000000000
27	6.63833260273973, 0.995749890410959
28	6.63833260273973, 0.995749890410959
29	6.65751853881279, 0.998627780821917
30	7, 98902224657534, 0.998627780821917
31	6.54240292237443, 1.00652352651914

Table 41 Significant Periods of Pass 159

1	6.67718684931507, 1.00157802739726
2	6.65848328767123, 0.998772493150685
3	1.00438356164384
4	0.97988640160374
5	6.65848328767123, 0.974412188439693
6	5.72330301369863, 1.00157802739726
7	6.69589041095890. 1.00438356164384
8	6.69589041095890. 1.00438356164384
9	0.97988640160374
10	1.00157802739726

Table 42 Significant Periods of Pass 170

1	1.00157802739726
2	1.00438356164384
3	1.00438356164384
4	1.00438356164384
5	1.00438356164384
6	1.00438356164384
7	1.00438356164384
8	1.03013698630137
9	1.03013698630137
10	1.00438356164384
11	1.00438356164384
12	1.00438356164384
13	1.00438356164384
14	1.00438356164384
15	1.03013698630137
16	1.00438356164384
17	1.03013698630137
18	1.02725951527924
19	1.02725951527924
20	1.02725951527924
21	6.67718684931507, 1.00157802739726
22	6.67718684931507, 1.00157802739726
23	6.69589041095890. 1.00438356164384
24	6.69589041095890. 1.00438356164384
25	6.69589041095890. 1.00438356164384
26	6.67718684931507, 1.00157802739726
27	6.67718684931507, 1.00157802739726
28	6.69589041095890. 1.00438356164384
29	6.69589041095890. 1.00438356164384
30	6.69589041095890. 1.00438356164384
31	6.69589041095890. 1.00438356164384
32	6.69589041095890. 1.00438356164384
33	8.03506849315069, 1.00438356164384
34	6.65848328767123, 0.974412188439693
35	6.65848328767123, 0.998772493150685

Table 43 Significant Periods of Pass 246

1	0.979886401603742
2	1.00438356164384
3	1.00438356164384
4	1.03013698630137
5	1.03013698630137
6	0.977118369528901
7	0.979886401603742
8	0.979886401603742
9	0.979886401603742
10	2.11449170872386, 1.03013698630137
11	1.03013698630137
12	2.11449170872386, 1.03013698630137
13	0.977118369528901
14	1.03013698630137
15	0.979886401603742
16	0.974350310725025
17	1.00438356164384
18	0.977118369528901
19	1.03013698630137
20	6.69589041095890, 1.03013698630137
21	6.69589041095890, 0.979886401603742
22	6.69589041095890, 0.979886401603742
23	0.979886401603742
24	6.69589041095890, 1.00438356164384
25	6.69589041095890.1.00438356164384, 0.9798864016037
26	8,01237063013699,1.00154632876712
27	6.69589041095890, 1.00438356164384
28	7.98967254794521, 0.998709068493150

APPENDIX H

Leading Three Spatial Models of Variability of Chosen Clusters
(68, 159, 170, and 246 respectively)

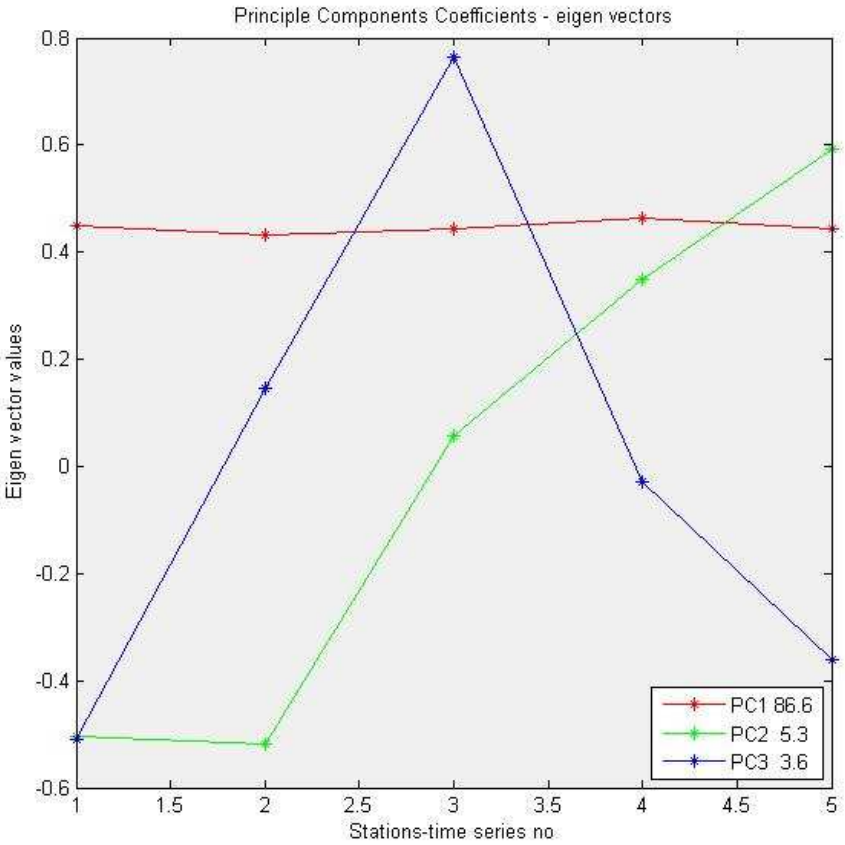

Figure 21 Leading Spatial Models for Pass 68

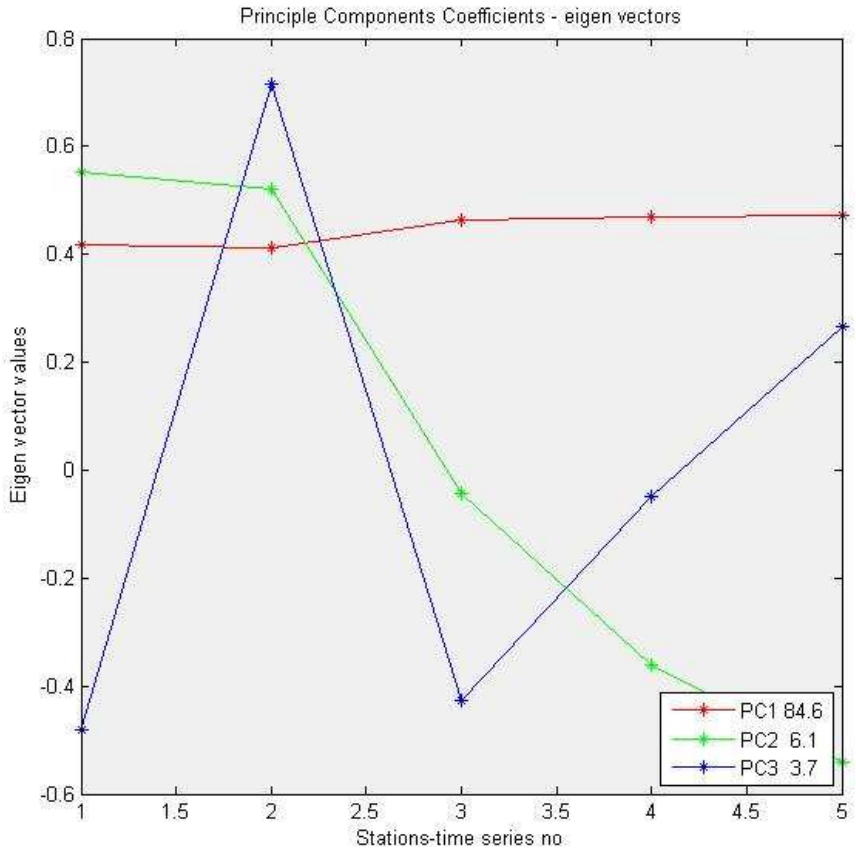

Figure 22 Leading Spatial Models for Pass 159

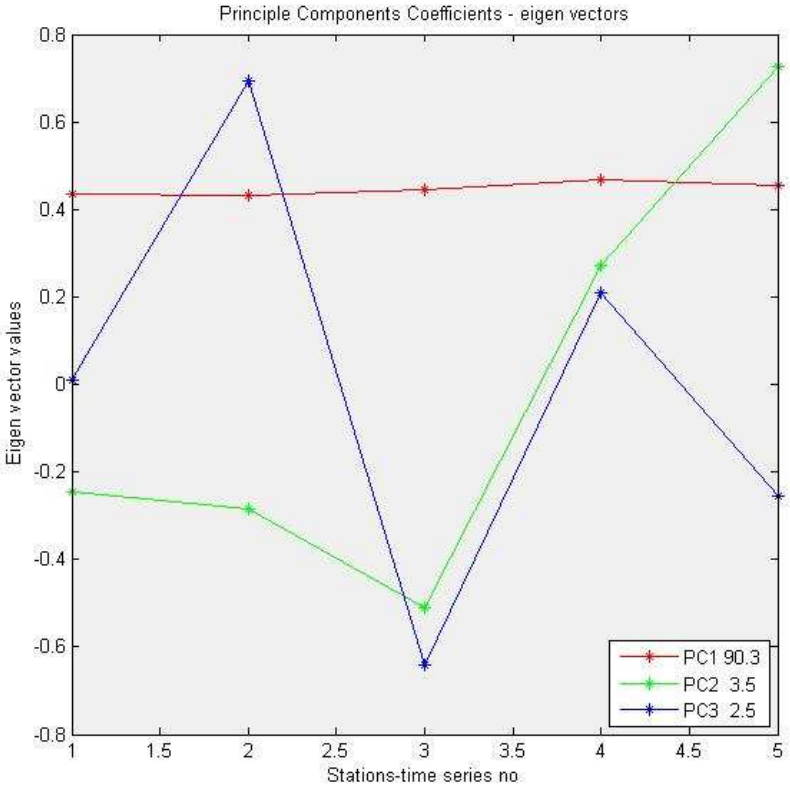

Figure 23 Leading Spatial Models for Pass 170

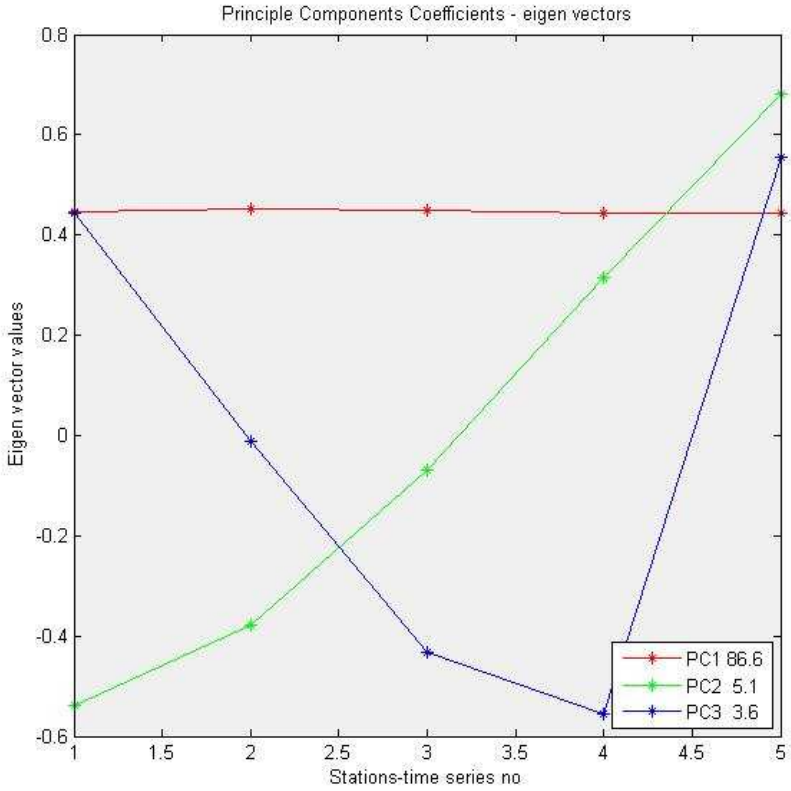

Figure 24 Leading Spatial Models for Pass 246